Applied Energy 341 (2023) 120912

Contents lists available at ScienceDirect

Applied Energy

journal homepage: www.elsevier.com/locate/apenergy

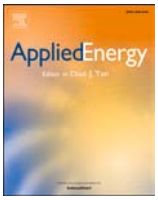

Assessment of capital expenditure for fixed-bottom offshore wind farms using probabilistic engineering cost model

Yuka Kikuchi, Takeshi Ishihara *

The University of Tokyo, School of Engineering, Department of Civil Engineering, Japan

HIGHLIGHTS

- A probabilistic engineering cost model is proposed to predict mean and standard deviation of CAPEX for offshore wind farms.
- The predicted CAPEX for the offshore wind farms with monopile foundations show good agreement with these reported in the UK.
- The cost reduction scenarios and the predicted supply prices agree well with those reported at the first auction in Japan.

ARTICLE INFO

Keywords:
Fixed-bottom offshore wind farm
Capital expenditure
Engineering cost model
Uncertainty
Cost reduction scenarios in Japan

ABSTRACT

The capital expenditure (CAPEX) for the fixed-bottom offshore wind farm is assessed using a probabilistic engineering cost model and the cost reduction scenarios in Japan are analyzed. Firstly, the engineering cost model is described to assess the capital expenditure. A new export cable length model is also proposed considering the landing point distance and the vessel size model is proposed as the function of turbine rated power. The proposed engineering cost model succeeds in explaining the mechanism of the increase and decrease of CAPEX experienced in the UK. The uncertainties of model parameters are identified from the reported data and modeled by the normal distribution function. The workability is predicted using the discrete event simulation. The predicted CAPEX is then compared with the existing 30 fixed-bottom offshore wind farms in the United Kingdom. The predicted mean and standard deviation values of CAPEX show good agreement with the reported ones, while the conventional parametric model underestimates the mean value and cannot predict the standard deviation. Finally, the cost reduction scenarios and their uncertainties of offshore wind farms in Japan are analyzed using the proposed probabilistic engineering cost model. The levelized cost of wind energy reduced from 20.0 JPY/kWh to 17.0 JPY/kWh, 13.6 JPY/kWh and 10.1 JPY/kWh by the reduction of installation days using the specific installation vessel, the turbine enlargement and the improvement of operation and maintenance efficiency. The predicted supply prices for each cost reduction scenario agree well with those reported at the first auction conducted in 2021 in Japan.

1. Introduction

In Japan, the sea area is the 6th worldwide and the offshore wind energy potential is 1600 GW [1]. In 2020, the government declared the installation target of 10 GW by 2030 and 30–45 GW by 2040 [2] for offshore wind. At the end of 2019, the installed capacity of offshore wind energy is 0.2 GW. In 2021, the first-round auction for the fixed-bottom offshore wind has been started with the capped feed-in tariff of 29 JPY/kWh (29 c$/kWh) [3]. The levelized cost of energy (LCOE) was calculated as 20 JPY/kWh (20 c$/kWh). It needs to be reduced to 8–9 JPY/kWh [2] in the early 2030s to achieve the installation target. The capital expenditure (CAPEX) was reported as 492 million JPY/kW, which was almost two times higher than that in Europe [3]. In the United Kingdom, the installation of offshore wind farm has started in the early 2000s, and the CAPEX increased once from 2009 to 2013, and reduced from 2014 to 2020. The cost reduction scenarios in Japan need to be analyzed by applying the cost reduction mechanism experienced in Europe.

IEA Task26 showed the structure of capital expenditure cost for offshore wind farm [4] and its representative price as a baseline in 2010. Crown Estate also published the representative cost structures in 2010 and 2019 for offshore wind farm [5,6]. The detailed cost elements are listed up for 100 wind turbines of 5 MW and 10 MW wind turbine,

* Corresponding author.
E-mail addresses: kikuchi@bridge.t.u-tokyo.ac.jp (Y. Kikuchi), ishihara@bridge.t.u-tokyo.ac.jp (T. Ishihara).

https://doi.org/10.1016/j.apenergy.2023.120912
Received 4 September 2022; Received in revised form 17 January 2023; Accepted 23 February 2023
Available online 24 April 2023

respectively. The CAPEX is mainly consisted of development and project management, wind turbine, balance of plant and installation. In 2012, the total CAPEX was described as 3070£/kW at 20 m water depth and 100 km far from shore, where development and project management cost is 120£/kW (4 % of the total CAPEX), wind turbine cost is 1200 £/kW (39 %), balance of plant cost is 940£/kW (31 %) and installation cost (26 %) is 810£/kW. In 2019, the total CAPEX was described as 2377 £/kW, where development and project management cost is 120£/kW (5 %), wind turbine cost is 1001£/kW (42 %), balance of plant cost is 605 £/kW (25 %) and installation cost is 651£/kW (27 %). The CAPEX is affected by the geographical conditions, such as water depth and distance from shore, and the wind farm configuration, such as turbine rated power and turbine number. In order to evaluate the CAPEX considering these effects, the cost model is required. The cost model is mainly categorized into the parametric cost model and the engineering cost model.

In the parametric cost model, the cost elements are modeled by the regression methods when the enough data are collected. The CAPEX for onshore wind farm in Japan was modeled by the parametric model with the input parameter of mean elevation, the maximum tilt angle, the distance to the construction road, the distance to the transmission line [7]. National Renewable Energy Laboratory [8] modeled the turbine cost with the input parameter of turbine rated power. European Environment Agency [9] constructed the CAPEX with the input of water depth and distance from shore. Gonzalez-Rodriguez [10] collected the data and showed the cost function with the capacity by a fitting curve. Shafiee et al. [11] proposed the detailed parametric cost model for the offshore wind farms. Alsubal et al. [12] recently assessed the cost of energy for offshore wind fam in Malaysia based on the cost model proposed by Shafiee et al [11], but the environmental condition difference is not considered when the parametric model built in Europe to the other country. In civil engineering field, machine learning methodology has been adopted recently for the cost estimation as the advanced methodology of the parametric models. Bayaram et al. [13] used multilayer perception and radial bases function using artificial neural network methods. Uncuoglu et al. [14] compares the prediction accuracy of several machine learning methodologies. However, the parametric model cannot be built in Japan yet, since there are only two demonstration project experiences [15] at Choshi with one 2.4 MW wind turbine on gravity based foundation and at Kitakyushu with one 2.0 MW wind turbine on jacket foundation, and one commercial offshore wind farm with 33 wind turbines of 4.2 MW on monopile foundation at Noshiro and Akita port area [16].

The cost elements in the engineering cost model are evaluated by the bottom-up approach. Each cost element is calculated based on the physical conditions. WindPACT project [17] was conducted for the turbine design. The engineering cost model was proposed by TU delft OWEC program [18] with the aim of the structure optimization of the fixed-bottom offshore wind turbine. The UK potential of offshore wind was also investigated using the engineering cost model [19–21]. ORE Catapult [22] showed the cost reduction scenario for the offshore wind farms using their in-house cost model and also investigated the technological progress observed for fixed-bottom offshore wind in the EU and UK [23]. WINDSPEED project [24] in Europe also developed a cost model to decide the use purpose of the North Sea. Nielsen [25] conducted the feasibility study from the engineering approach. Dicorato et al. [26] modelled the offshore wind farm investment costs and carried out the cost analysis for a 150 MW offshore wind farm. Ioannou et al. [27] gave the sensitivity study and the insights regarding potential minimum asking and maximum offered price. They developed a parametric CAPEX, Operational expenditure (OPEX) and LCOE expressions from the simulated cost using the engineering cost model [27] for ease of use. National Renewable Energy Laboratory (NREL) also developed the engineering cost models called as SeaBOSSE and ORBIT [28,29]. Shields et al. [30] investigated the sensitivity of wind turbine rated power and wind farm size on the CAPEX using their cost models. They also investigated the spatial impacts in the United States [31]. Gaglayan et al. [32] evaluated the offshore wind energy potential in Europe using those cost models proposed by NREL. Kaiser and Synder [33] proposed the cost model for installation. However, the power transmission system is not well formulated in the previous engineering cost models, although the export cable length differs significantly depending on whether the landing point is near or far. For the installation cost model, the vessel day rate has a major impact, but the day rate is constant value and it is not a function of turbine rated power in the previous model. When turbine rated powers become larger, the required vessels need to be bigger, which leads the day rate increase. The day rate needs to be a function of turbine rated power.

The uncertainty of CAPEX is an important issue for the engineering applications. In the previous studies, the uncertainty of the installation cost has been studied well. Muhabie et al. [34] analyzed the installation procedure using the discrete event simulation. Paterson et al. [35] assessed the installation process for the UK offshore rounds 1 and 2. ECN Install [36], ORBIT [28,29] and Shoreline [37] is well-known tools for the discrete event simulations. In the simulations, the weather prediction of wind and wave is very important. Kikuchi and Ishihara [38] conducted the discrete event simulation using simulated wind and wave time series to show the workability difference between the two demonstration projects in Japan. The simulation accuracy is improved by many researchers such as Kikuchi et al. [39], Başakın et al. [40]. Muhabie et al. [41] investigated the effect of stochastic parameters on the offshore wind farms assembly strategies using the discrete-event simulation. The uncertainty of LCOE is firstly investigated by Ozkan et al. [42] developing a comprehensive system model of offshore wind farm. The cable cost, substation cost, network connection and SCADA cost were considered as a triangular distribution, and the weather downtime due to the bad weather was expressed as the PERT distribution. However, those uncertainties were not based on the reported value because there was not enough data at that time. Ioannou et al. [43] presented the stochastic prediction of offshore wind farm LCOE, where the coefficient of variation of CAPEX was estimated from the existing databases, while the number of parameters was limited. Therefore, the uncertainty of CAPEX needs to be assessed comprehensively.

Various studies of cost reduction scenario have been conducted. The first major study named as “offshore wind cost reduction pathways study” was conducted by the Crown Estate [44], which was based on the comprehensive industrial interview approach. ORE Catapult [45] continued research and assessed a cost reduction scenario considering technology innovation. A series of cost models and basic data sets were built to improve the analysis of the impact of innovations on future offshore wind costs was named as DELPHOS tool. Beiter et al. [29] combined more detailed engineering cost model and DELPHOS tools and assessed the cost reduction scenario during 2015–2030 in the United States. ORE Catapult performed the cost reduction analysis for fixed-bottom and floating offshore wind farm using the engineering cost model [45,46]. However, the uncertainty in the cost reduction scenario was not evaluated by the engineering cost model since the deterministic cost model were used in these studies.

In summary, the export cable length and installation vessel need to be modelized and the predicted CAPEX by the engineering cost model needs to be validated. The uncertainty of cost element needs to be evaluated using the probabilistic engineering cost model. The cost reduction scenario and its uncertainty need to be assessed in Japan.

In this study, the CAPEX of the fixed-bottom offshore wind farms in the United Kingdom is analyzed using probabilistic engineering cost model and the cost reduction scenarios in Japan is investigated. The probabilistic engineering cost model used in this study are described and the new cost model of export cable length and installation vessel size are proposed in Section 2. The parameters in the engineering cost model and those uncertainties are identified from the database of the fixed-bottom offshore wind farms, and the proposed probabilistic engineering cost model is validated with the reported data of UK offshore wind farms

Finally, the cost reduction scenario in Japan and its uncertainty are investigated and are validated by the first auction results at the end of 2021. Conclusions are summarized in Section 4.

2. Methodology

Data collection of fixed-bottom offshore wind farm in this study is described in Section 2.1. The engineering cost model for the fixed-bottom offshore wind farm and uncertainty evaluation methodology used in this study is described in Section 2.2. The cost reduction scenario analysis methodology is explained in Section 2.3.

2.1. Data collection of fixed-bottom offshore wind farm

In this study, the various dataset is used for the parameter identification and validation. Table 1 shows the input and output parameters of the probabilistic engineering cost model proposed in this study and their nomenclatures. The input parameter is water depth, distance from shore, number of turbines and the turbine rated power. The output parameter is CAPEX obtained as the summation of various cost elements, which is defined in Section 2.2 with the listed equations. For the validation process conducted in Section 3.2.6, 4C Offshore database [47] is used. 4C Offshore database [47] includes the water depth, distance from shore, number of turbines, turbine rated power and CAPEX data. The results obtained by analyzing those data are shown in Figs. 8, 9, 21, 22 as listed in Table 1.

The model parameters of the proposed probabilistic engineering cost model are summarized in Table 2. The model parameters for each cost element and their nomenclature are also shown in this table. The type of parameter is described as deterministic of 1 or probabilistic of 2. Some parameters are considered deterministic, though they should be probabilistic, because the reported data is not available. The reported data of the existing wind farm are used to identify those parameters in Section 3.2. The references of those reported data are also listed up in Table 2. The turbine cost data are collected from Crown Estate [5,6], ODE [19], Sieros et al. [48] and the technical reports from National Renewable Energy Laboratory [49–55]. The diameter, length and thickness of monopile are obtained from Negro et al. [56]. The wind farm layout information is obtained from kingfisher wind farms charts published by "The Kingfisher Information Service – Offshore Renewable & Cable Awareness project" [57]. The number of array cables are counted visually from those detailed wind farm layout data. The export cable length, the number of export cable, the distribution-ends voltage, the number of offshore substation, the array cable length, and the main host capabilities of vessels are collected from 4C Offshore database [47]. The installation days for one turbine and substructure are captured from Lacal-Arantegui et al. [58]. Historical data for steel, copper and fuel prices refers to the U.S Bureau of Labor Statistics [59–61] for the unit steel cost for substructure model and the unit export and array cable cost. The numbers of the figures for each model parameter are listed in Table 2.

All cost data in this study is 2019 year value considering the inflation rate and the currency exchange described in world bank's database [62] following the previous study [63].

2.2. Probabilistic engineering cost model

The engineering cost models for CAPEX are used in this study. The mean value of CAPEX is evaluated by the conventional engineering cost models, while the model parameters are updated to reflect the recent technological advances. In addition, the number of input variables is reduced for validation and scenario study.

The cost breakdown structure for the offshore wind farms was defined by Shafiee et al. [11]. The cost structure used in this study is described in Fig. 1. CAPEX consists of three main items: the development and consenting cost $C_{D\&C}$, the production and acquisition cost $C_{P\&A}$, and the installation and commissioning cost $C_{I\&C}$ as shown in Equation (1).

$$CAPEX = C_{D\&C} + C_{P\&A} + C_{I\&C} \tag{1}$$

The development and consenting cost consists of project management cost C_{projM}, legal authorization cost C_{legal}, the engineering cost C_{eng}, the contingencies $C_{contigencies}$ and the surveys $C_{surveys}$, which is described in Section 2.2.1. The production and acquisition cost consists of the wind turbine cost C_{WT}, the support structure cost C_{SS} and the power transmission system cost C_{PTS}, which is investigated in Section 2.2.2. The installation and commissioning cost consists of the vessel cost $C_{I\&C,vessel}$,

Table 1
Input and output parameters of the proposed probabilistic engineering cost model and reference.

Input and output parameter	Nom.	Equation	Figure	Ref.
Input				
Water depth	h_w		Fig. 9	[47]
Distance from shore	d_{shore}		Fig. 9	[47]
Number of turbines	N_{WT}		Fig. 9	[47]
Turbine rated power	P_{WT}		Fig. 9	[47]
Output				
Capital expenditure	CAPEX	Eq. (1)	Figs. 8, 21, 22	[47]
Development and consenting cost	$C_{D\&C}$	Eq. (2)		
Production and acquisition cost	$C_{P\&A}$	Eq. (3)		
Wind turbine cost	C_{WT}	Eq. (3-1)		
Support structure cost	C_{SS}	Eq. (3-2)		
Power transmission cost	C_{PTS}	Eq. (3-3)		
Export cable cost	C_{EC}	Eq. (3-3-1)		
Offshore substation cost	$C_{off-subs}$	Eq. (3-3-2)		
Array cable cost	C_{AC}	Eq. (3-3-3)		
Onshore cable cost	C_{OC}	Eq. (3-3-4)		
Onshore substation cost	$C_{on-subs}$	Eq. (3-3-5)		
Installation and commissioning cost	$C_{I\&C}$	Eq. (4)		
Vessel cost	$C_{I\&C,vessel}$	Eq. (4-1)		
Mobilization cost	$C_{vessel,mob,i}$	Eq. (4-1-1)		
Fuel cost	$C_{vessel,fuel,i}$	Eq. (4-1-2)		
Installation cost	$C_{vessel,install,i}$	Eq. (4-1-3)		
Port cost	$C_{I\&C,port}$	Eq. (4-2)		
Other cost	$C_{I\&C,others}$	Eq. (4-3)		

Table 2
Model parameters of the proposed probabilistic engineering cost model and references.

Model parameter	Nom.	Type	Figure	Ref.
Development and consenting cost model				
Fixed development and consenting cost	$c_{D\&C,fixed}$	1		[5]
Survey cost per MW	c_{survey}	1		[5]
Wind turbine cost model				
Wind turbine cost per MW	c_{WT}	2		[5,6,19,48–55]
Substructure cost model				
Unit steel cost per ton	$c_{ss,steel}$	2		[59]
Production cost per ton	$c_{ss,production}$	1		[5]
Diameter of substructure	d_{SS}	2	Fig. 13 (a)	[56]
Length of substructure	l_{SS}	2	Fig. 13 (b)	[56]
Thickness of substructure	t_{SS}	2	Fig. 13 (c)	[56]
Density of steel	ρ_{Steel}	1		–
Power transmission cost model				
Unit export cable cost per length	c_{EC}	2		[60]
Export cable length	l_{EC}	2	Fig. 14 (a), (b)	[47]
The number of export cable	N_{EC}	1	Fig. 14 (c)	[47]
Distribution-ends voltage	V_{EC}	1	Fig. 15 (a)	[47]
The number of offshore substation	$N_{off-subs}$	1	Fig. 16 (b)	[47]
Unit cost of offshore substation per turbine	$c_{off-subs}$	1		[5]
The number of array cable	N_{AC}	1	Fig. 15 (b)	[57]
Array cable length	l_{AC}	2	Fig. 17 (b)	[47]
Unit array cable cost per length	c_{AC}	2		[60]
Onshore cable length	l_{OC}	2		–
Unit onshore cable cost	c_{OC}	1		–
Installation and commissioning cost				
Main host capabilities of vessels	$A_{vessel,i}$	1	Fig. 18 (a), (b)	[47]
The fuel price	$c_{vessel,fuel,i}$	2		[61]
The number of stuffs per one trip	$N_{transort,i}$	1		–
The distance from the installation port	$d_{port,i}$	1		–
Installation vessel cost	$c_{vessel,i}$	1		[5]
Installation day	$T_{install,i}$	2	Fig. 19(a), (b)	[58]
Workability	α_i	2		–
Port cost per turbine	$c_{I\&C,port}$	1		–
Other cost per turbine	$c_{I\&C,others}$	1		–

Values for which no existing data are available, are evaluated as constants in this study.
1 Deterministic parameter.
2 Probabilistic parameter: The uncertainty is evaluated in Section 3.2 based on the existing values.

the port cost $C_{I\&C,port}$ and other cost $C_{I\&C,others}$ including insurance, which is discussed in Section 2.2.3.

2.2.1. Development and consenting cost

The development and consenting cost $C_{D\&C}$ is evaluated using Equation (2) as defined by Shafiee et al. [11]. It is related to the project management C_{projM}, the legal authorization C_{legal}, the engineering activities C_{eng}, the contingencies $C_{contigencies}$ and the conducted surveys $C_{surveys}$.

$$C_{D\&C} = C_{projM} + C_{legal} + C_{eng} + C_{contigencies} + C_{surveys} \tag{2}$$

In this study, the summation of C_{projM}, C_{legal}, C_{eng}, $C_{contigencies}$ is estimated as a constant value $C_{D\&C,fixed}$ in Equation (2–1) as shown in Table 4 even though these items for each project are slightly difficult. $C_{surveys}$ is proportional to the wind farm capacity as shown in Equation (2–2).

$$C_{projM} + C_{legal} + C_{eng} + C_{contigencies} = C_{D\&C,fixed} \tag{2-1}$$

$$C_{surveys} = c_{surveys} P_{WT} N_{WT} \tag{2-2}$$

where P_{WT} is the wind turbine rated power, N_{WT} is the number of turbines, $c_{surveys}$ is the survey cost per MW as shown in Table 4.

2.2.2. Production and acquisition cost

The production and acquisition cost includes all costs associated with the procurement of wind turbines C_{WT}, the support structure or foundation C_{SS}, and the power transmission system C_{PTS}.

$$C_{P\&A} = C_{WT} + C_{SS} + C_{PTS} \tag{3}$$

The total cost of wind turbine C_{WT} is expressed as a function of the number of wind turbines and the wind turbine rated power. Shafiee et al. [11] modeled the wind turbine cost for 2 MW to 5 MW wind turbines, which does not cover the recent turbines larger than 6 MW.

Physically, the mass of wind turbine is the cube of the length and the power is the square of the length, so that the ratio of mass to power is proportional to the length. However, the technological improvement suppresses the mass and leads the mass to be proportional to the rated power as mentioned by Sieros et al [48]. Up to 6 MW, the cost per MW increases in proportion to rated power. On the other hand, for recent turbines larger than 7 MW, the industry practice shows that the wind turbine cost per kW becomes constant. This is because the further technological innovation occurs in the lighter blade material, the advanced generator and gearbox. It also relates with the business model shift in the turbine manufactures. Currently the manufactures contract not only turbine supplies but also operation of turbines for steady and predictable cash flow, which leads the turbine cost reduction.

In this study, the wind turbine cost per MW is modeled as proportional to rated power until 6 MW and constant after 7 MW as shown in Equation (3-1).

$$C_{WT} = \begin{cases} \left(c_{wt,1} P_{WT} + c_{wt,2}\right) P_{WT} N_{WT} \ , & P_{WT} < 6\text{MW} \\ \left(c_{wt,3} P_{WT} + c_{wt,4}\right) P_{WT} N_{WT} \ , & 6\text{MW} \le P_{WT} < 7\text{MW} \\ c_{wt,5} P_{WT} N_{WT} \ , & 7\text{MW} \le P_{WT} \end{cases} \tag{3-1}$$

The wind turbine cost between 6 MW and 7 MW is linearly interpolated, which does not affect the cost estimation because there is no wind turbine model between 6 MW and 7 MW. It is assumed that the transportation costs are included in this study. Turbine costs are negotiated for individual project and are usually kept confidential by suppliers and developers, and so there are uncertainties and are modeled in

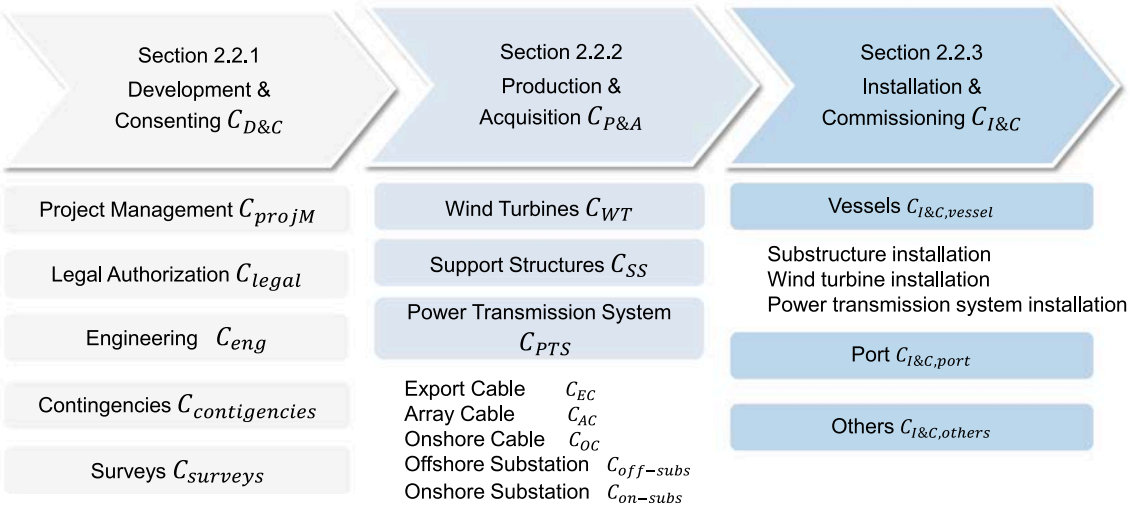

Fig. 1. Cost breakdown structure for offshore wind farms.

Section 2.3. The coefficients from $c_{wt,1}$ to $c_{wr,5}$ are identified using the database as shown in Table 5.

For the substructure cost C_{SS}, Nielsen [25] and Dicorato et al. [26] investigated the sensitivity of substructure cost to the water depth. WINDSPEED project [24] and ORBIT project [28,29] evaluated the substructure cost using the engineering model as shown in Equation (3–2).

$$C_{SS} = W_{ss}\left(c_{ss,\,steel} + c_{ss,\,prodction}\right) \tag{3-2}$$

Here,

$$W_{ss} = \pi d_{ss} t_{ss} l_{ss} \rho_{steel} N_{WT} \times 1.25$$

$$d_{ss} = \max\left(4,\ 0.0003h_w^2 + 0.0627h_w + 3.9687\right)$$

$$t_{ss} = a_{ss,1}h_w + a_{ss,2}$$

$$l_{ss} = a_{ss,3}h_w + a_{ss,4}$$

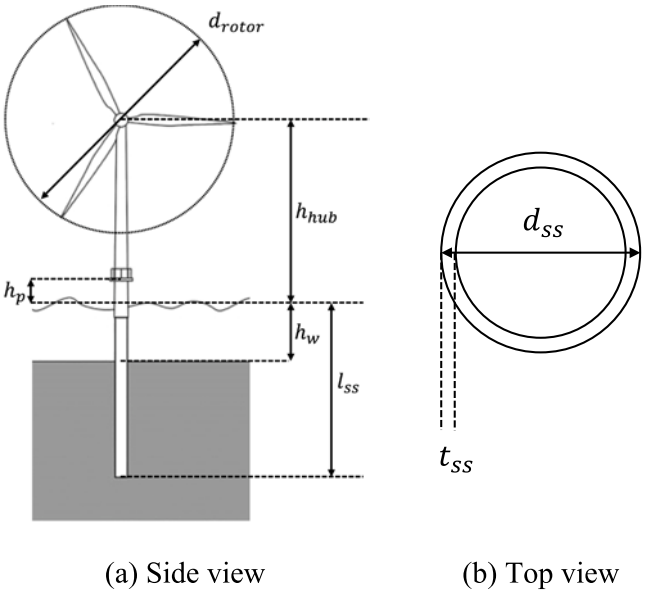

Fig. 2. Schematic of support structure.

where the substructure cost is calculated from the weight of monopole W_{ss} and the summation of unit steel price $c_{ss,steel}$ and unite manufacturing $c_{ss,prodction}$. The volume of hollow cylinder is calculated from the diameter d_{ss}, the length l_{ss} and the thickness t_{ss} of monopile as shown in Fig. 2. h_w is the water depth of the site. The coefficients from $a_{ss,1}$ to $a_{ss,4}$ are identified using the database as shown in Table 6.

In WINDSPEED project [24], the preliminary design of monopile was conducted for different water depth and significant wave height, and the monopile cost was derived by curve fitting as a function of water depth for each significant wave height. In ORBIT model [28,29], the monopile of diameter, thickness and length is scaled with rotor diameter, hub height of wind turbine and water depth. Van der Tempel [64] derived a formula for the monopile diameter using the equation of tower 1st mode to avoid the resonance of rotor rotation with structures as a design criteria of monopile. ODE [19] also modeled the monopile diameter using this approach. This study follows Tempel's methodology. The diameter d_{ss} is calculated as the function of water depth. The minimum diameter is set as 4 m due to the restriction of the size of commercial offshore wind turbines. The thickness t_{ss} is thought to be proportional to the water depth due to the static pressure. The length of monopile l_{ss} consists of the water depth h_w, the embedded length and the upper part from the water level, and it is also modeled as a function of the water depth.

For the power transmission system cost C_{PTS}, it is composed of the export cable cost C_{EC}, the offshore substation cost $C_{off-subs}$, the array cable cost C_{AC}, the onshore cable cost C_{OC} and the onshore substation cost $C_{on-subs}$ as shown in Equation (3–3).

$$C_{PTS} = C_{EC} + C_{off-subs} + C_{AC} + C_{OC} + C_{on-subs} \tag{3-3}$$

Fig. 3 illustrates the structure of power transmission system cost models used in this study. The performance of the proposed models are validated in Section 3.2.2.

WINDSPEED project [24] used the packing density concept and the turbine spacing was modeled as a function of its packing density, however, the methods for the evaluation of the export cable length, the number of export cables are not clear. In this study, the input variables are limited to distance from shore, capacity, number of turbines, water depth, rated power and used to calculate the export cable cost as shown in Equation (3–3-1). The export cable length is modeled depending on whether the landing point is near or far.

The offshore substation cost model is proposed as shown in Equation (3–3-2) to consider the cable length gap defined as the difference in the length of export cable with and without offshore substation in this study. When the cable length gap is larger than 30 km per one turbine and wind

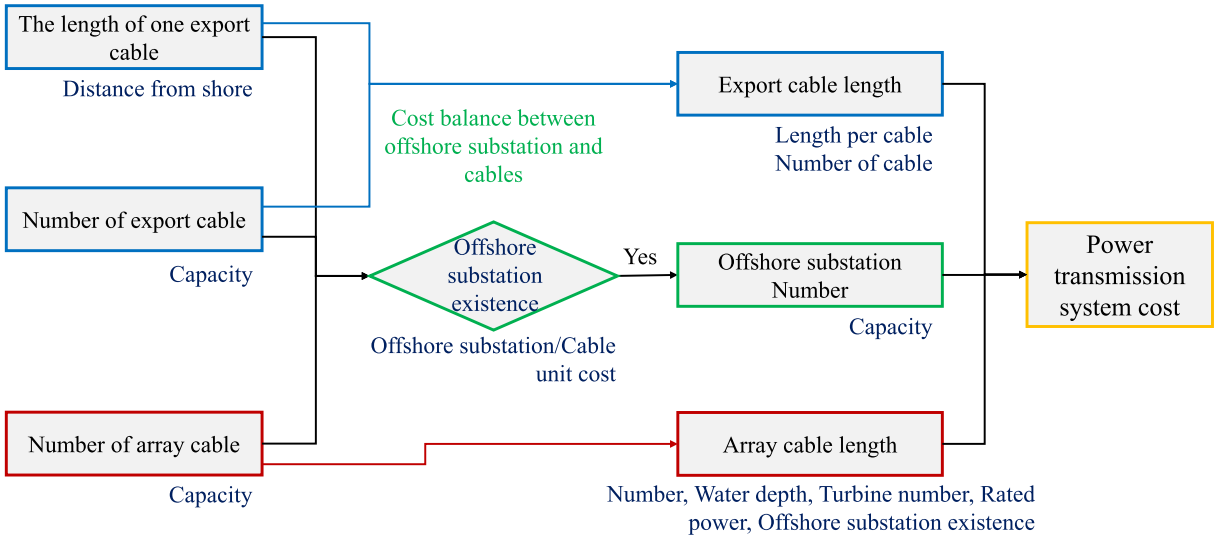

Fig. 3. The structure of power transmission system cost model.

farm capacity is larger than 500 MW, the offshore substation will be built.

NREL ORBIT model [28,29] calculated the array cable cost C_{AC} from the detailed power calculation model with the input parameters of plant capacity, turbine rated power, rotor diameter, turbine spacing, row spacing, water depth, cable rated voltage, current capacity, AC resistance, inductance capacitance. However, these parameters are difficult to be identified for each specific site. In this study, the distance from shore and the wind farm capacity are used as the input variables to calculate the array cable cost C_{AC} as shown in Equation (3-3-3).

The export cable cost C_{EC} is evaluated as the product of the length of export cable l_{EC}, the unit export cable cost c_{EC} and the number of export cables N_{EC} as shown in Equation (3-3-1).

$$C_{EC} = l_{EC} c_{EC} N_{EC} \tag{3-3-1}$$

Here,

$$l_{EC} = \begin{cases} l_{EC,near} = a_{EC,1} d_{shore} + a_{EC,2}, \ \Delta l_{EC} < 5 \text{ km} \\ l_{EC,far} = a_{EC,1} d_{shore} + a_{EC,3}, \ \Delta l_{EC} \geq 5 \text{ km} \end{cases}$$

$$\Delta l_{EC} = d_{landfall} - d_{shore}$$

$$P(\Delta l_{EC} < 5 \text{ km}) = P_1, \ P(\Delta l_{EC} \geq 5 \text{ km}) = P_2$$

$$N_{EC} = \left\lceil \frac{P_{WT} N_{WT}}{1.2 V_{EC}} \right\rceil$$

$$V_{EC} = 132 \ kV$$

where l_{EC} is the export cable length, c_{EC} is the export cable cost per km and is assumed as a constant, d_{shore} is the distance from shore, N_{EC} is the number of export cables. V_{EC} is the distribution-ends voltage, Δl_{EC} is the difference between the distances from the land fall point and from the shore point.

The export cable length l_{EC} depends on whether the land fall point is near or far from the shore point as shown in Fig. 4. The export cable requires the extra length to allow the cable displacement due to the wave and earthquake and to maintain ease of installation. The extra length is generally about 10 % of the total cable length. The other extra length is also needed at the starting and the ending part of the cable. Considering these aspects, the export cable length l_{EC} is evaluated by a linear function of the distance from shore d_{shore} when the land fall point is near the shore point and Δl_{EC} is shorter than 5 km. Otherwise, when the land fall point is far from the shore point and Δl_{EC} is longer than 5 km, an extra length is added in $a_{EC,3}$. The probability of Δl_{EC} less than 5 km and that more than 5 km are identified in Section 3.2.1. The coefficients from $a_{EC,1}$ to $a_{EC,3}$ are identified using the database as shown in Table 7.

The number of export cables N_{EC} is calculated by dividing the wind farm capacity by the distribution-ends voltage of export cable V_{EC}, which is assumed as 132 kV in this study. The value of 1.2 is decided by the regression analysis.

Note that the number of export cables should be the number of

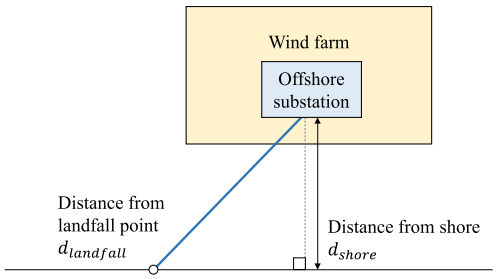

Fig. 4. Schematic of export cable and land fall point.

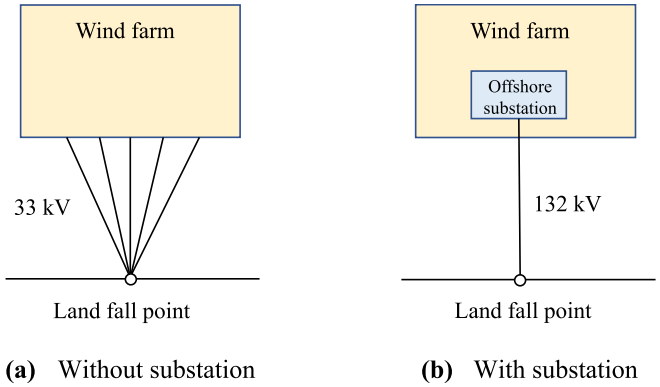

Fig. 5. Schematic of export cable and offshore substation.

offshore substation in the case of wind farms with substations and the export cable cost should be the array cable cost in the case of wind farms without substations.

The offshore substation cost $C_{off-subs}$ is evaluated by Equation (3–3-2). The number of array cable N_{AC} is calculated by dividing the wind farm capacity by the distribution-ends voltage of array cable V_{AC}. The transmission capacity of the array cable is generally proportional to the distribution-ends voltage of array cable. The distribution -ends voltage is modeled as 33 kV for the 2 ~ 9 MW wind turbines and 66 kV for the wind turbine larger than 9 MW.

$$C_{off-subs} = N_{off-subs} c_{off-subs} \tag{3-3-2}$$

Here,

$$l_{AC} = \begin{cases} \kappa\{\beta_1 d_{rotor}(N_{WT} - N_{AC}) + (h_w + h_p)(2N_{WT} - N_{AC})\}, & N_{off-subs} = 0 \\ \kappa\{\beta_2 d_{rotor}(N_{WT} - N_{AC}) + XN_{AC} + (h_w + h_p)(2N_{WT} - N_{AC})\}, & N_{off-subs} \geq 1, radial \\ \kappa\{\beta_3 d_{rotor}(N_{WT} - 0.5N_{AC}) + XN_{AC} + (h_w + h_p)(2N_{WT})\}, & N_{off-subs} \geq 1, ring \end{cases}$$

$$V_{AC} = \begin{cases} 22 \text{ kV}, & P_{WT} \leq 2\text{MW} \\ 33 \text{ kV}, & P_{WT} \leq 9\text{MW} \\ 66 \text{ kV}, & P_{WT} \leq 15\text{MW} \end{cases}$$

$$N_{off-subs} = \begin{cases} 0, & \Delta l_{PTS} < 55 \text{ km} \\ \left\lceil \frac{P_{WT} \times N_{WT}}{500} \right\rceil, & \Delta l_{PTS} \geq 55 \text{ km} \end{cases}$$

$$\Delta l_{PTS} = l_{EC}(N_{AC} - N_{EC})$$

$$N_{AC} = \lceil P_{WT} N_{WT} / V_{AC} \rceil$$

where $N_{off-subs}$ is the number of substation, $c_{off-subs}$ is the cost of offshore substation. Δl_{PTS} is the difference in the length of export cable with and without offshore substation, and V_{AC} is the distribution ends voltage of array cable and modeled as the function of turbine rated power. The number of offshore substation $N_{off-sub}$ is evaluated from the breakeven point where the offshore substation cost equals to the reduced export cable cost. The schematic of the export cables with and without the offshore substation are depicted in Fig. 5 (a) and (b), respectively. The cable length gap Δl_{PTS} is defined as the difference in the length of export cable with and without offshore substation. When the cable length gap Δl_{PTS} becomes more than 55 km per one turbine, the offshore substation platform will be considered and one offshore substation will be built per 500 MW wind farm capacity based on the experience.

For the offshore substation cost $C_{off-subs}$, WINDSPEED project [24] and ORBIT model [28,29] proposes the detailed engineering cost model for substation considering topside, reactors, switchgears, ancillary systems, substation assembly cost, cost of substation substructure. Gonzalez-Rodriguez [10] mentioned that substation costs increase with capacity. In this study, one substation cost per turbine $c_{off-subs}$ is assumed as a constant value.

The array cable cost C_{AC} is evaluated by multiplying the cable length l_{AC} by the cable cost per unit c_{AC} as shown in Equation (3-3-3). The schematics of array cable for the radial and ring topologies are shown in Fig. 6 (a) and (b).

$$C_{AC} = l_{AC} c_{AC} \tag{3-3-3}$$

Here,

$$d_{rotor} = \sqrt{\frac{P_{WT}}{0.0003}}$$

where l_{AC} is the length of array cable and the unit is meter, c_{AC} is the cost of array cable per meter, d_{rotor} is the diameter of the rotor, N_{AC} is the array cable number and h_p is the length between sea surface and tower bottom.

The array cable length l_{AC} is divided into the link between turbines, the link between turbine and offshore substation, and the inside of the turbine, which corresponds to the first, second and third term in the equations respectively. This equation depends on whether there is an offshore substation and whether the cable layout bases is the radial or ring topology. In this study, the ring topology is assumed. The distance between turbines is evaluated as a function of $\beta_i d_{rotor}$ and the rotor diameter is modeled as a function of the turbine rated power. The distance between the turbine and the offshore substation X is modeled as 1.5 times of the distance between turbines. $\beta_i (i = 1, 2, 3)$ is determined by the regression analysis. $\beta_1 = 5$ is used for offshore substation non-existence case, and $\beta_2 = \beta_3 = 7$ is used for offshore substation existence case. κ is assumed as 1.2. h_p is the length between seawater surface and tower bottom as shown in Fig. 2 (a) and is assumed as 20 m. The unit of length is meter.

The onshore cable cost C_{OC} is evaluated as shown in Equation (3–3-4). In this study, the length of onshore cable length l_{ON} is considered as a constant value and the coefficient is identified from the database.

$$C_{OC} = l_{OC} c_{OC} \tag{3-3-4}$$

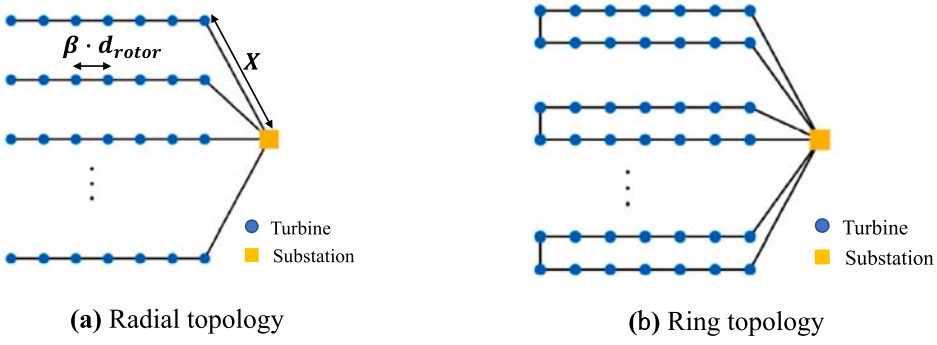

(a) Radial topology **(b)** Ring topology

Fig. 6. Schematic of array cable.

The onshore substation cost $C_{on\text{-}subs}$ is expressed as proportional to the wind farm capacity and evaluated as shown in Equation (3-3-5).

$$C_{on\text{-}subs} = C_{on\text{-}subs} P_{WT} N_{WT} \tag{3-3-5}$$

where $C_{on\text{-}subs}$ is assumed as a constant value as shown in Table 7.

2.2.3. Installation and commissioning cost

As mentioned in the previous studies [24,28], the installation cost

$$A_{vessel,i} = \begin{cases} W_1, & P_{WT} < 3.6\,\mathrm{MW} \\ P_1 = \dfrac{exp(W_1)}{exp(W_1)+exp(W_2)}, P_2 = \dfrac{exp(W_2)}{exp(W_1)+exp(W_2)}, & P_{WT} = 3.6\,\mathrm{MW} \\ W_2, & 3.6\mathrm{MW} < P_{WT} \le 10\mathrm{MW} \\ W_3, & 10\mathrm{MW} < P_{WT} \end{cases}$$

$C_{I\&C}$ is composed of the vessel cost $C_{vessel,install}$, port cost $C_{I\&C,port}$ and the other cost $C_{I\&C,others}$ as shown in Equation (4).

$$C_{I\&C} = C_{I\&C,vessel} + C_{I\&C,port} + C_{I\&C,others} \tag{4}$$

The vessel cost $C_{I\&C,vessel}$ is composed of mobilization cost $C_{vessel,mob,i}$, fuel cost $C_{vessel,fuel,i}$, installation cost $C_{vessel,install,i}$ for each installation phase i as shown in Equation (4-1).

$$C_{I\&C,vessel} = \sum_{i=1}^{n}\left(C_{vessel,mob,i} + C_{vessel,fuel,i} + C_{vessel,install,i}\right) + C_{vessel,install,AC} + C_{vessel,install,EC} + C_{install,Off-Subs} N_{off-subs} + C_{install,On-Subs} P_{WT} N_{WT} \tag{4-1}$$

Mobilization cost $C_{vessel,mob,i}$ is expressed in Equation (4-1-1) and is considered as the mobilization cost as the 1 % of installation cost in WINDSPEED project [24].

Fuel cost $C_{vessel,fuel,i}$ for wind turbines (WT) and support structures (SS) is calculated as the product of the total distance of transportation and the fuel price per one kilometer $c_{vessel,fuel,i}$ in Equation (4-1-2). The total distance of transportation is calculated by multiplying the distance from port $d_{port,i}$ and the round-trip numbers. The round-trip numbers are evaluated as the division of the total number of wind turbine N_{WT} to the number of the stuffs per one trip $N_{transport,i}$ that can be loaded on one vessel. $A_{vessel,i}$ expresses the vessel size factor and is explained below.

Installation cost $C_{vessel,install,i}$ for wind turbines and support structures is calculated as the vessel rate per day $c_{vessel,install,i}$ multiplied with the total installation days in Equation (4-1-3). Total installation days are calculated by multiplying the installation days $T_{install,i}$ per one installation phase i by the number of wind turbines N_{WT}. The transportation time per one-way trip is calculated as the distance from port $d_{port,i}$ divided by the vessel speed $V_{vessel,i}$. The number of trip is calculated as the number of wind turbines divided by the number of stuffs per one trip that can be loaded on one vessel. Workability α_i is considered as the ratio of available working time to the total construction time for each installation phase i.

A vessel size factor $A_{vessel,i}$ is newly defined as a function of turbine rated power in this study since the vessel size has been increased to accommodate larger wind turbines and improve installation efficiency recently and discussed in Section 3.2.3. types of the vessels are used for these wind turbines. The vessel size factor is calculated based on the crane size of the vessel, and discussed in Section 3.2.

$$C_{vessel,mob,i} = 0.01 C_{vessel,install,i} \tag{4-1-1}$$

$$C_{vessel,fuel,i} = A_{vessel,i} c_{vessel,fuel,i}\left(2\left\lceil\frac{N_{WT}}{N_{transport,i}}\right\rceil d_{port,i}\right) \tag{4-1-2}$$

$$C_{vessel,install,i} = A_{vessel,i} c_{vessel,install,i}\left(2\left\lceil\frac{N_{WT}}{N_{transport,i}}\right\rceil\left\lceil\frac{d_{port,i}}{24 V_{vessel,i}}\right\rceil + N_{WT} T_{install,i}\right)\Big/\alpha_i \tag{4-1-3}$$

Here,

The cost of array ($C_{vessel,install,AC}$) and export cable installation vessels ($C_{vessel,install,EC}$) are difficult to obtain publicly. In this study, the models proposed in WINDSPEED project [24] as shown Equation (4–1-4) and Equation (4–1-5) are used. The parameters are shown in Table 8.

$$C_{vessel,install,AC} = c_{install,AC} l_{AC} \tag{4-1-4}$$

$$C_{vessel,install,EC} = c_{install,EC} l_{EC}\ N_{EC} \tag{4-1-5}$$

The port cost $C_{I\&C,port}$ is assumed to be proportional to the turbine numbers as shown in Equation (4-2). The other cost $C_{I\&C,others}$ is also estimated as a function of the turbine numbers as shown in Equation (4-3). Since this cost component involves insurance and construction project management, it is assumed to be proportional to the project scale, reflected with the number of turbines. This component is further assumed to be included for the projects commissioned in 2014 onwards based on the Crown Estate statement [6].

$$C_{I\&C,port} = c_{I\&C,port} N_{WT} \tag{4-2}$$

$$C_{I\&C,others} = c_{I\&C,others} N_{WT} \tag{4-3}$$

2.2.4. Evaluation of uncertainty in models

In this study, the uncertainties of model parameter in the probabilistic engineering cost model are approximated by the normal distribu-

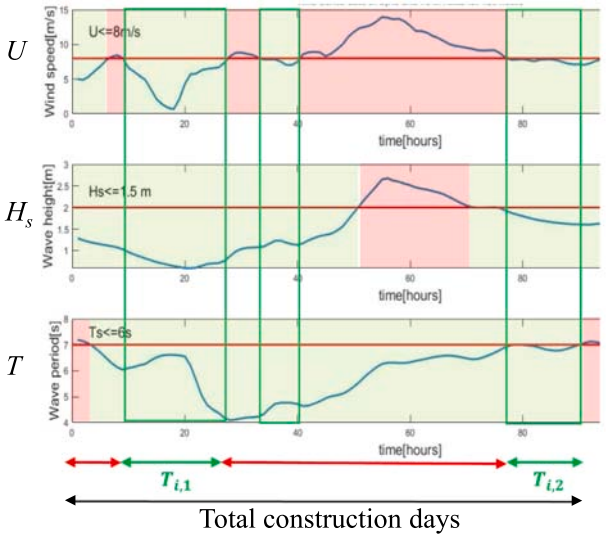

Fig. 7. Schematic of workability assessment.

tions as shown in Ioannou et al. [27]. The mean value μ_{actual}, standard deviation σ_{actual} and coefficient of variance (CoV) of each model parameter are evaluated using Equations (5) – (7).

$$\mu_{actual} = \sqrt{\frac{\sum_{i=1}^{N_{data}} x_{actual,i}}{N_{data}}} \tag{5}$$

$$\sigma_{actual} = \sqrt{\frac{\sum_{i=1}^{N_{data}} \left(x_{actual,i} - x_{model,i}\right)^2}{N_{data}}} \tag{6}$$

$$CoV = \frac{\sigma_{actual}}{\mu_{actual}} \tag{7}$$

where, $x_{actual,i}$ is the reported value for model parameter *i*. $x_{model,i}$ is the predicted value by the engineering cost model. CoV is assumed to be a constant for each parameter and identified using the collected database in the study as shown in Table 9.

Each model parameter is evaluated by performing Monte Carlo simulation and approximated as the normal distribution, because it is mostly evaluated by the product of each parameter based on the central limit theorem. The goodness of normal distribution fitness is assessed by Kolmogorov-Smirnov test using a significance level of 0.05. In this study, the mean, the standard deviation and the arbitrary quantile of CAPEX for each wind farm are evaluated by the proposed probabilistic engineering cost model.

2.2.5. Workability assessment

The uncertainty of workability is assessed by the discrete event simulation. The workability α varies from year to year due to the weather conditions. The workability is assessed by the discrete event simulation according to the following order for various years. The time series data for the weather conditions are prepared as $x_j(t)$ for the weather condition j, such as wind speed, wave height, wave period or current speed. When $x_j(t)$ is less than the workable limitation $x_{j,limit}$, the time is counted as the workable time. When all weather conditions are workable, the time is then counted as the workable. The summation of continuous workable time is counted as a workable weather window. The workable weather window T_i needs to be larger than the minimum required installation time for one travel $T_{required,min}$. The counting is continued till the total workable time $T_{workable}$ to reach the total required installation time $T_{required,total}$. Finally, the total installation period is calculated and the workability α is defined as the ratio of total workable days to the total construction days. These processes are depicted in Fig. 7.

The time series data for the weather conditions are simulated by the numerical models. The constructed simulation tools were validated at two demonstration projects in Japan as mentioned in Kikuchi and Ishihara [38]. The predicted workability matches well with the reported workability.

$$\alpha = \frac{T_{workable}}{\text{Total construction days}} \tag{8}$$

Here,

$$T_{workable} = \sum T_i, \ \ if \ \ T_{workable} < T_{required,total}$$

$$T_i = \sum Y(t) \ > \ T_{required,min}$$

$$Y(t) = \begin{cases} 1, \ if(X_1(t) = 1) \cap (X_2(t) = 1) \cap \cdots \cap (X_j(t) = 1) \\ 0, \ if(X_1(t) = 0) \cup (X_2(t) = 0) \cup \cdots \cup (X_j(t) = 0) \end{cases}$$

$$X_j(t) = \begin{cases} 1, \ if \ x_j(t) \le x_{j,limit} \\ 0, \ if \ x_j(t) > x_{j,limit} \end{cases}$$

2.3. Study of cost reduction scenarios in Japan

The installed offshore wind farm capacity in Japan is 7.4 MW with 3 turbines in the end of 2021, excluding near-shore offshore wind farm of 44.2 MW [65]. All of 3 turbines were installed for the demonstration projects. The first commercial offshore wind farm at the Akita and Noshiro port area with 140 MW (33 turbines of 4.2 MW) has been operated since the end of 2022 [16].

To promote the development of offshore wind in Japan, the "Act on Promoting Utilization of Sea Areas for Development of Power Generation Facilities Using Maritime Renewable Energy Resources" was enforced in April 2019. The promotional zone of offshore wind farm and the developer are decided through the auction [66]. The first auction was conducted in 2021 for three fixed-bottom offshore wind farms. The auction sites are 'Noshiro city, Mitane cho, Oga city offshore in Akita prefecture', 'Yurihonjo offshore in Akita prefecture' and 'Choshi offshore in Chiba prefecture'. The auction is planned annually and aims to select developers for 10 GW offshore wind farms by 2030 and the target LCOE is 8–9 JPY/kWh.

However, the LCOE in 2020 in Japan is 20 JPY/kWh and the cap of tariff is 29 JPY/kWh based on the government announcement. This LCOE was assessed for the four sites: Akita Nosiro, Santane and Oga offshore, Akita Yurihonjo offshore North side, Akita Yurihonjo offshore South side, Chiba Choshi offshore sites. Those area was selected for the first auction in Japan. The average wind speed of four sites is 7.56 m/s, which leads the capacity factor of 33.2 %. The water depth is 18.6 m, which is the mean value of maximum and minimum water depths. The distance from shore is set as 6 km based on the mean value of four sites. Wind turbine rated power and turbine number are set as 10 MW and 37. CAPEX and OPEX are estimated as 51.2 Million JPY/MW and 1.84 Million JPY/MW/year. Decommissioning expenditure (DECEX) is estimated as 10.7 Million JPY/MW, which is assessed as 80 % of installation cost in CAPEX. The availability, electricity loss, wake loss and other loss is set as 95 %, 3.1 %, 10 %, 3.0 %, respectively. The operation year is set as 20 years in Japan.

To achieve the target LCOE of 8–9 JPY/kWh, the cost reduction scenarios at the different phases in Japan are proposed during 2024–2030 in this study. The mean value and standard deviation are evaluated using the proposed probabilistic engineering cost model for each cost reduction scenario. The standard cost of 20 JPY/kWh in 2020 in Japan is used as a baseline. The input values of engineering cost model, such as turbine rated powers and installation days are determined based on the literature review from the industry. The sensitivity study for CAPEX with installation days and turbine rated powers is conducted, where CAPEX is estimated by using the proposed engineering cost model for various installation days and turbine rated powers. The mean value and standard deviation of LCOE and supply price are

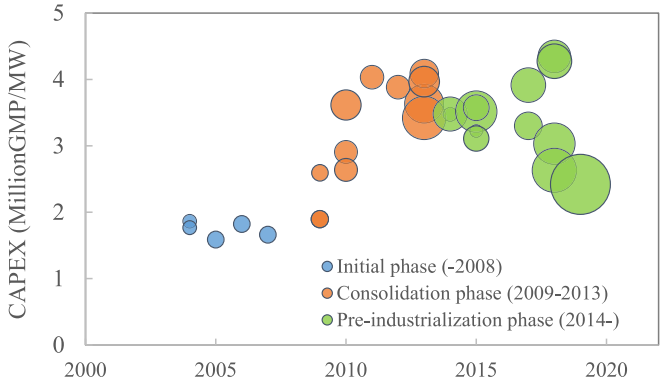

Fig. 8. The change in capital expenditure for UK offshore wind farm with monopile foundations by year of installation. The bubble size represents the wind farm capacity.

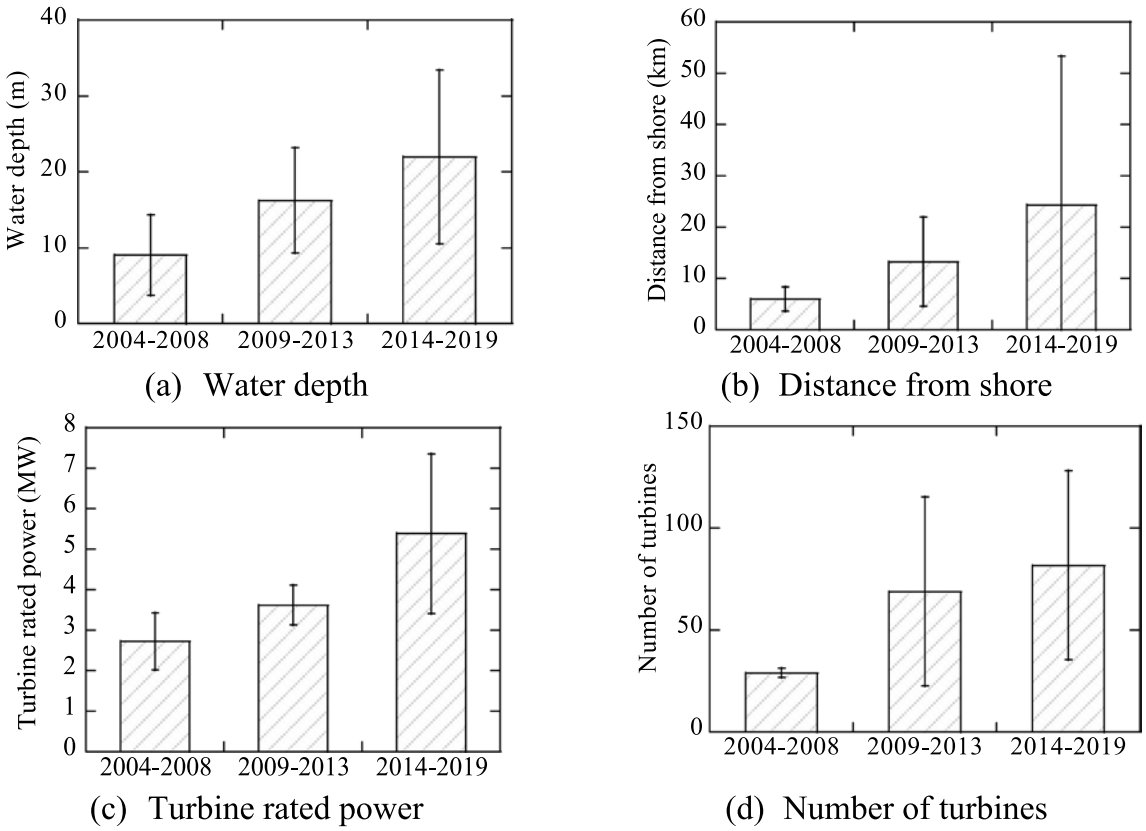

Fig. 9. Transition of UK offshore wind farms.

Table 3
Conditions inputted for each phase of UK offshore wind industry (* denotes assumption).

Phase	Capacity (MW)	Turbine rated power (MW)	Number of Turbines	Water depth (m)	Distance from Shore (km)
UK Initial (-2008)	79	2.7	29	8.65	6.38
UK consolidation (2009–2013)	249	3.6	69	16.23	13.27
UK pre-industrialization (2014–2020)	818	10*	82	21.98	24.33
UK 2020s	1227	15*	82	21.98*	24.33*

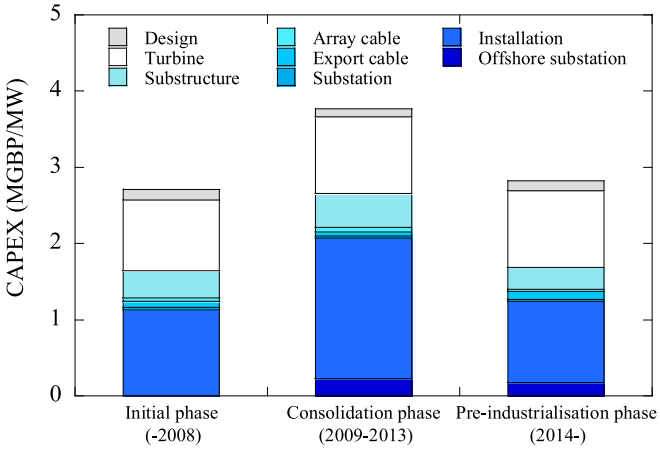

Fig. 10. The predicted CAPEX for each phase.

evaluated using the proposed probabilistic engineering cost model. The feasibility of the proposed cost reduction scenarios is validated using the first auction for three offshore wind farms in Japan conducted in 2021.

3. Results and discussion

Database is built from the collected references and the CAPEX in each development phase is analyzed by by the proposed engineering model in Section 3.1. The parameter ineach cost model are identified from the database in Section 3.2. The uncertainty of each cost parameter and workability are evaluatedand the proposed enginnering cost model is validated with the reported CAPEX.The CAPEX reduction scenarios of offshore wind in Japan are analyzed and compared with the first auction results in Japan in Section 3.3.

3.1. Analysis of cost data and reduction mechanism

The database is built from the collected references described in Section 2.1. The change in CAPEX for UK offshore wind farm with monopile foundations by year of installation is shown in Fig. 8. The offshore wind farms are categorized into the initial phase before 2008, the consolidation phase from 2009 to 2013, and the pre-industrialization from 2014 as defined by Lacal-Arantegui et al. [58]. The transition of offshore wind farms such as water depth, distance from shore, turbine rated power and number of turbines in those three phases are plotted in Fig. 9, where bar graphs show mean values and error bars denote standard deviations. It is obvious that the CAPEX increases in the consolidation phase and reduces in the pre-industrialization phase,

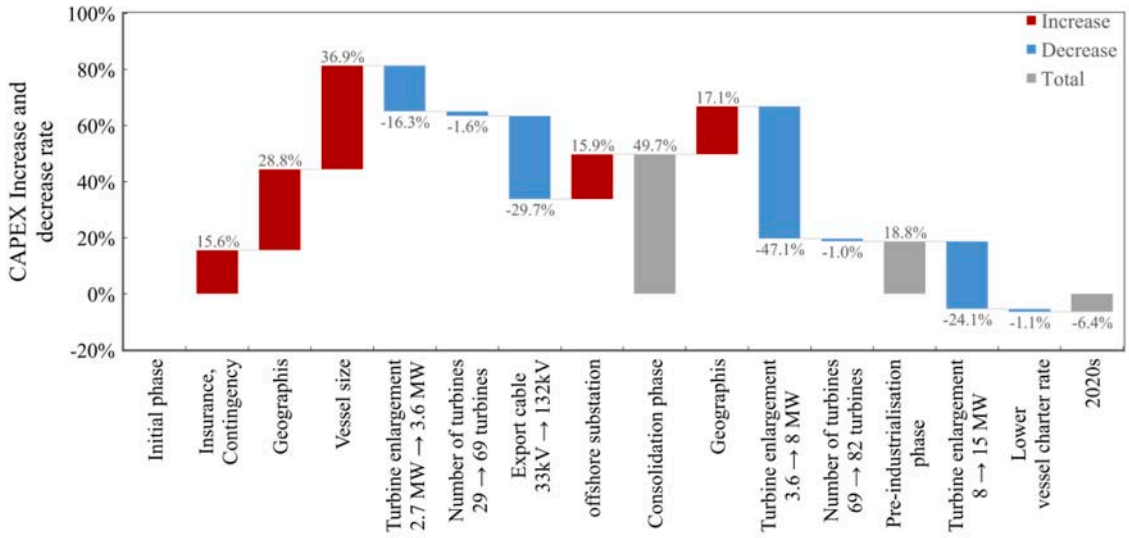

Fig. 11. Water fall of cost transition.

Table 4
Identified parameters for development cost.

Model parameter	Nomenclature	Value	Unit	Equation
Fixed development cost	$C_{D\&C,fixed}$	3,684,373 (less than 300 MW) 23,378,000 (larger than 300 MW)	GBP GBP	Eq. (2–1)
Survey cost per MW	$c_{surveys}$	97,792	GBP/MW	Eq. (2–2)

Table 5
Identified parameters for wind turbine cost model.

Model parameter	Nomenclature	Value	Unit	Equation
Coefficient of wind turbine	$c_{WT,1}$	78,300	–	Eq. (3–1)
Coefficient of wind turbine	$c_{WT,2}$	717,000	–	do.
Coefficient of wind turbine	$c_{WT,3}$	−190,000	–	do.
Coefficient of wind turbine	$c_{WT,4}$	2,330,000	–	do.
Coefficient of wind turbine	$c_{WT,5}$	1,000,000	–	do.

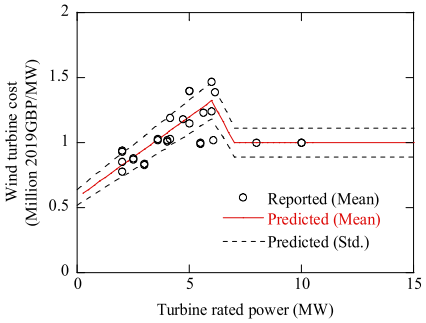

Fig. 12. Comparison of wind turbine costs predicted by the proposed model and reported data.

though water depth, distance from shore and wind farm capacities have continued to increase through these phases. The mechanism of these changes in CAPEX are discussed in this section.

The mechanism of change in CAPEX is analyzed using the proposed engineering cost model. The input parameters are the mean value for each phase as described in Table 3. Fig. 10 shows that the predicted CAPEX in each phase using the engineering cost model. The increase of CAPEX from the initial phase to the consolidation phase is well captured. The reduction of CAPEX from consolidation phase to pre-industrialization phase is also well explained.

Fig. 11 presents the water fall of cost transition. The increase of cost from the initial phase to the consolidation phase is due to the increase of the water depth and the distance from shore, while the cost reduction from consolidation phase to pre-industrialization phase is due to the increase of wind turbine capacity and the decrease of vessel rate are the main factor of this reduction. This indicates that the proposed engineering cost model can reproduce the increase and the decrease of CAPEX in each phase of offshore wind development. Note that upgrading vessel increases vessel day rate, but improves workability. From this analysis, it is found that the cost is firstly reduced by the improvement of construction efficiency and then by the increase of turbine capacity.

3.2. Identification of parameters in probabilistic engineering cost models

Each parameter of engineering cost model is identified based on the database described in Table 2. Other references are used as supplement and are described in the following sections.

3.2.1. Parameters for development cost

Parameters for development cost as shown in Equation (2-1) and (2-2) are identified from Crown Estate 2010 [5] as shown in Table 4. In development and consent costs, environmental survey, coastal process survey, metstation survey and seabed survey are counted as the survey cost. The other cost is counted as the fixed development cost.

3.2.2. Parameters for production and acquisition cost

Table 5 summarizes the parameters in the wind turbine cost model as shown in Equation (3–1), which are identified based on the reports by Crown Estate 2010 [5] and 2019 [6], Offshore Design Engineering Limited ODE [19] published in 2007, Sieros et al. [48], and the reports

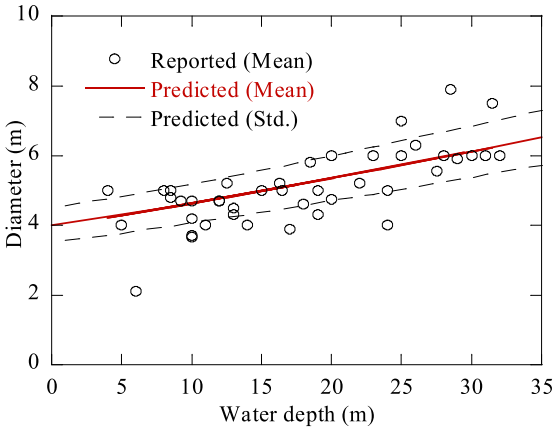

(a) Diameter of monopile

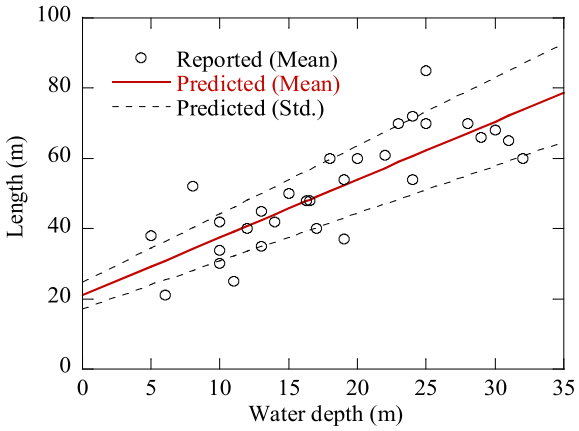

(b) Length of monopile

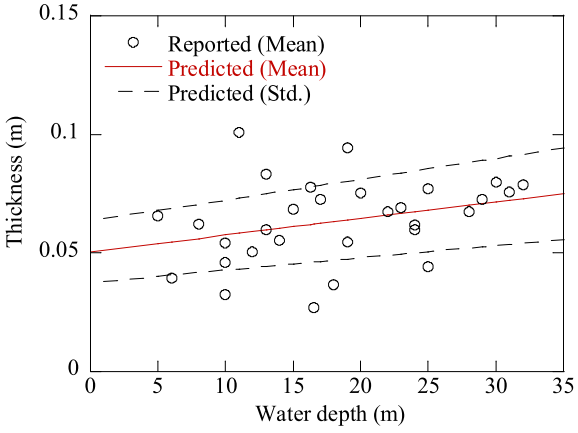

(c) Thickness of monopile

Fig. 13. Parameters of support structure cost model.

Table 6
Identified parameters for the substructure cost model.

Model parameter	Nomenclature	Value	Unit	Equation
Cost of steel per unit weight	$c_{ss,steel}$	0.91	GBP/kg	Eq. (3–2)
Cost of manufacturing per unit weight	$c_{ss,production}$	2.37	GBP/kg	do.
Density of steel	$\rho_{ss,steel}$	7,870	kg/m^3	do.
Coefficient for monopile thickness	$a_{ss,1}$	0.001	–	do.
Coefficient for monopile thickness	$a_{ss,2}$	0.05	–	do.
Coefficient for monopile length	$a_{ss,3}$	1.65	–	do.
Coefficient for monopile length	$a_{ss,4}$	21	–	do.

Table 7
Identified parameters for power transmission system cost models.

Model parameter	Nomenclature	Value	Unit	Equation
Onshore substation	$c_{on-subs}$	25,000	GBP/MW	Eq. (3–3-5)
Unit cable cost for export cable	c_{EC}	731,698	GBP/km	Eq. (3–3-1)
Coefficient for export cable length	$a_{EC,1}$	1.18	km	do.
Coefficient for export cable length	$a_{EC,2}$	0.92	km	do.
Coefficient for export cable length	$a_{EC,3}$	26.48	km	do.
Offshore substation	$c_{off-subs}$	58,445,000	GBP/turbine	Eq. (3–3-2)
The distribution-ends voltage of array cable	V_{AC}	22, 33, 66	kV	do.
Unit cable cost for array cable	c_{AC}	220,755	GBP/km	Eq. (3–3–3)
Distance parameter of array cable	κ	1.2	–	do.
Distance parameter of array cable	β_1	5	–	do.
	β_2	7	–	do.
	β_3	7	–	do.
Onshore cable length	l_{OC}	1	km	Eq. (3–3-4)
Unit cable cost for onshore cable	c_{OC}	731,698	GBP/km	do.

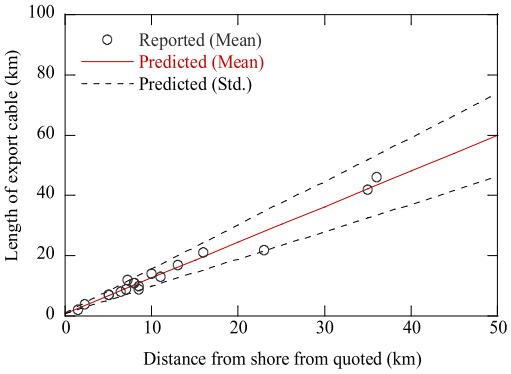

(a) Relationship between export cable length and distance from shore quoted for a nearby landfall point

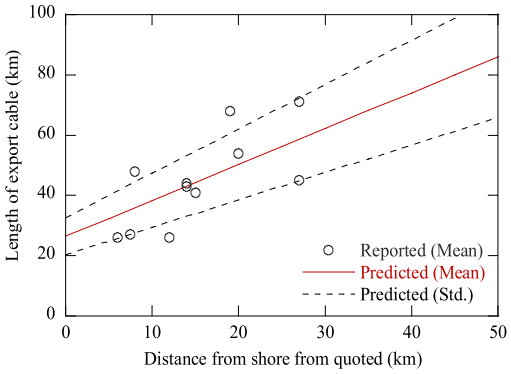

(b) Relationship between export cable length and distance from shore quoted for a distant landfall point

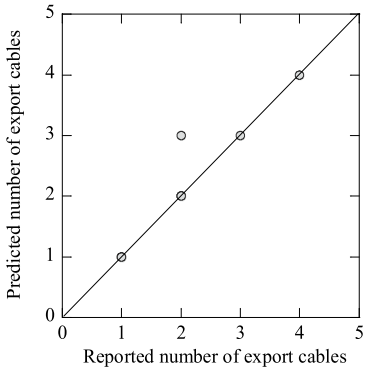

(c) Comparison of predicted and reported number of export cables

Fig. 14. Validation of export cable cost model.

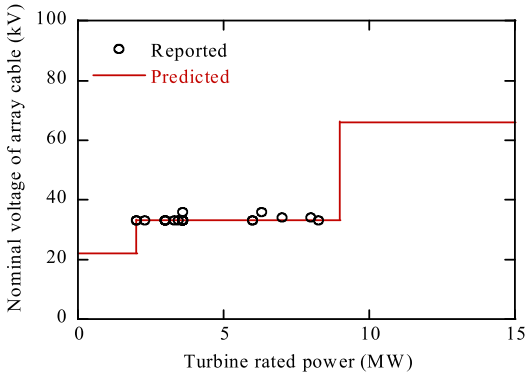

(a) Relationship between turbine rated power and distribution ends voltage

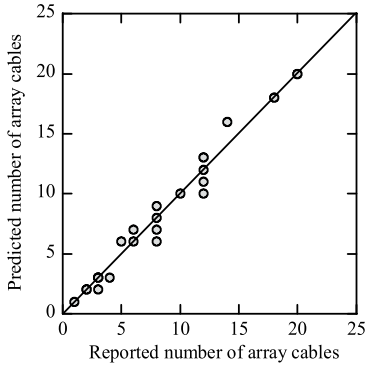

(b) Predicted and recorded array cable number

Fig. 15. Validation of model for number of array cables.

by NREL published from 2015 to 2020 [49–55]. Fig. 12 shows the predicted and reported wind turbine cost per MW by the proposed model. Dash lines show the standard deviation of the model, which is described in Section 3.2.4. As described in Section 2.2.2, the cost of turbine per MW increases up to 6 MW and levels off after 7 MW.

Fig. 13 shows the comparison of reported diameter, length and thickness with predicted ones by the proposed model. The predicted mean values of diameter derived theoretically agrees well with the reported ones. Table 6 summarizes the parameters in substructure cost models. The parameters for the length and thickness are identified from the database. The unit cost per ton is identified from the total cost of Crown Estate. The steel cost $c_{ss,steel}$ is identified from U.S. Bureau of Labor Statics [59]. The cost of manufacturing per unit weight is identified from the unit cost per ton and the steel cost.

The parameters for power transmission system are summarized in Table 7 and the parameters for export cable length is identified from the

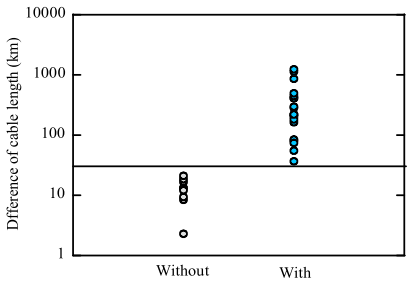

(a) Relationship between offshore substation existence and the cable length gap

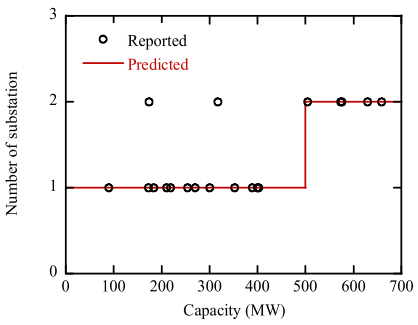

(b) Predicted and reported number of substations

Fig. 16. Validation of offshore substation model.

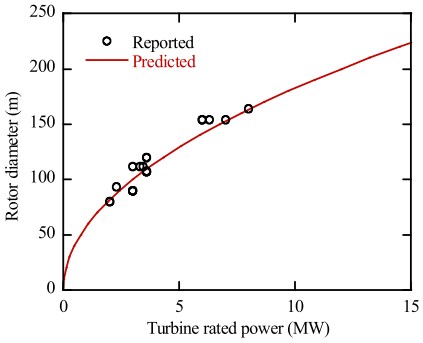

(a) Relationship between rotor diameter and rated power

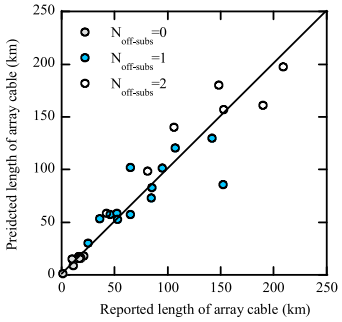

(b) Predicted and reported array cable length for different number of offshore substations

Fig. 17. Validation of array cable length.

Table 8
Identified cost parameters for installation cost.

Model parameter	Nomenclature	Value	Unit	Equation
Offshore substation installation cost	$C_{install,Off-Subs}$	11,689,000	GBP/substation	Eq. (4–1)
Onshore substation installation cost	$C_{install,On-Subs}$	25,000	GBP/MW	Eq. (4–1)
Vessel fuel cost for support structure	$c_{vessel,fuel,SS}$	333.33	GBP/km	Eq. (4–1-2)
Vessel fuel cost for wind turbine	$c_{vessel,fuel,WT}$	333.33	GBP/km	do.
Vessel cost for support structure	$c_{vessel,install,SS}$	315,603	GBP/day	Eq. (4–1-3)
Vessel cost for wind turbine	$c_{vessel,install,WT}$	315,603	GBP/day	do.
Vessel speed for support structure	$V_{vessel,SS}$	11	knots	do.
Vessel speed for wind turbine	$V_{vessel,WT}$	11	knots	do.
Installation day for support structure	$T_{install,SS}$	3.35	days/foundation	do.
Installation day for wind turbine	$T_{install,WT}$	3.60	days/turbine	do.
Array Cable installation cost	$c_{install,AC}$	662,266	GBP/km	Eq. (4–1-4)
Export cable installation cost	$c_{install,EC}$	975,393	GBP/km	Eq. (4–1-5)
Port cost per area	$c_{I\&C,port}$	146,000	GBP/turbine	Eq. (4–2)
Other installation cost	$c_{I\&C,others}$	2,120,000	GBP/turbine	Eq. (4–3)

reported export cable length. Fig. 14 (a) shows the relationship between the export cable length and the distance from shore quoted when the land fall point is near the shore point and Δl_{EC} is shorter than 5 km. The export cable length is well evaluated by a linear function of the distance from shore quoted. Fig. 14 (b) shows the relationship between the export cable length and the distance from shore quoted when the land fall point is far from the shore point and Δl_{EC} is longer than 5 km. The export cable length is evaluated by the same linear function with an extra length of 26 km. The uncertainty in the export cable length is much larger than those when the land fall point is near the shore point. The probability of Δl_{EC} less than 5 km and that more than 5 km are identified as P_1=0.61 and P_2=0.39 respectively from the reported data. The predicted number of export cables by Equation (3-3-1) matches well with the reported ones as shown in Fig. 14 (c).

The distribution-ends voltage of array cable V_{AC} in Equation (3-3-2) is 22 kV up to 2 MW, 33 kV up to 9 MW and 66 kV higher than 9 MW decided from the industry interview. The predicted and the reported nominal voltage are plotted in Fig. 15 (a). The predicted array cable numbers by Equation (3-3-2) match well with the reported ones as shown in Fig. 15 (b).

The relationship between offshore substation existence and the cable length gap is depicted in Fig. 16 (a). The predicted and reported number of substations are depicted as shown in Fig. 16 (b). The two exceptions are Robin rigg and Sheringham shoal wind farm. It is suggested that the

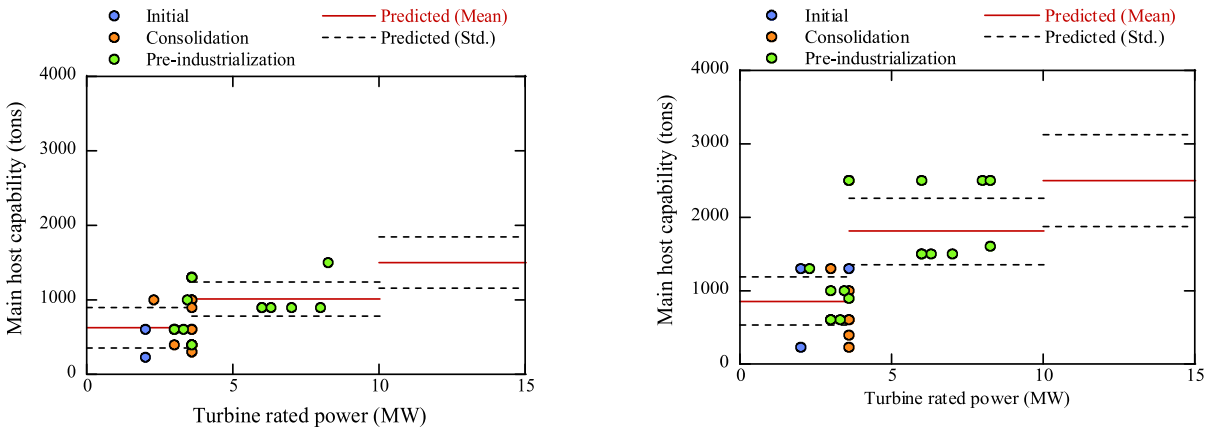

(a) Crane capacity of vessel for wind turbine installation

(b) Crane capacity of vessel for substructure installation.

Fig. 18. Main host capacity of installation vessel for each development phase.

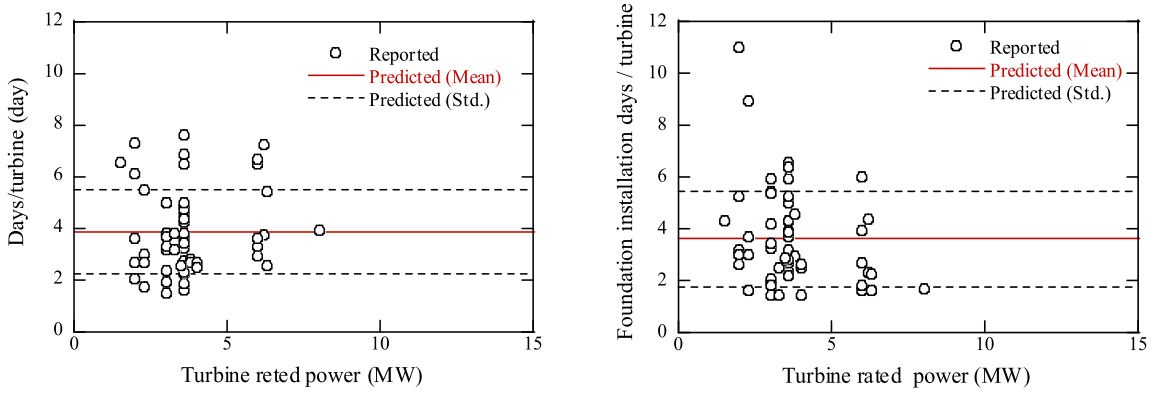

(a) Installation days for one turbine.

(b) Installation days for one substructure.

Fig. 19. Variation of installation days with turbine rated power.

redundancy may be emphasized in these two wind farms.

The distance between the first turbine and the offshore substation is modeled as 1.5 times of the distance between turbines. β is determined by the regression analysis and 5 for offshore substation non-existance case and 7 for offshore substation existence case. Fig. 17 (a) illustrates the relationship between the rotor diameter d_{rotor} and rating power described in Equation (3-3-3). Fig. 17 (b) shows the predicted and reported array cable length for different number of offshore substations $N_{off-subs}$.

3.2.3. Parameters for installation and commisioning cost

The parameters for installation and commissioning test are summarized in Table 8. The vessel size is modelized as a function of turbine rated power in this study. From database, the relationship between the main host capabilities with wind turbine rated power are plotted in Fig. 18 for wind turbine installation and that for substructure installation. It is found that vessels can be categorized into three groups: less than3.6 MW, between 3.6 MW and 10 MW, and greater than 10 MW.

The vessel size factor $A_{vessel,i}$ is determined by the ratio of the average main host size, with 1 being the group of wind turbines larger than 3.6 MW and less than 10 MW. For wind turbine installation vessel, the average main host size is 1009 ton The wind turbine installation vessels for 10 MW or more have not yet been reported yet. Installation vessels of 1500 tons are assumed. For substructure installation vessels, the average main host size is 1810 tons. No substructure installation vessels for wind turbines of 10 MW or larger have yet been reported. Installation vessels of 2500 tons are assumed to be used from the planed wind farms.

The installation vessels for 3.6 MW wind turbine are divided into two groups due to the high demand of offshore wind farm installation at the time. The vessel size factor is determined by the logit model. Occurrence rate P_1 using small vessels and P_2 using large vessels are determined as a percentage of the reported number of vessels used. Occurrence rates P_1 and P_2 are respectively 2/3 and 1/3 for wind turbine installation vessels as shown in Equation (9) and 4/9 and 5/9 for substructure installation vessels as shown in Equation (10).

$$A_{vessel,WT} = \begin{cases} 0.62, & P_{WT} < 3.6\,\mathrm{MW} \\ P_1 = \frac{2}{3}, P_2 = \frac{1}{3}, & P_{WT} = 3.6\,\mathrm{MW} \\ 1, & 3.6MW < P_{WT} \leq 10MW \\ 1.49, & 10MW < P_{WT} \end{cases} \tag{9}$$

$$A_{vessel,SS} = \begin{cases} 0.47, & P_{WT} < 3.6\,\mathrm{MW} \\ P_1 = \frac{4}{9}, P_2 = \frac{5}{9}, & P_{WT} = 3.6\,\mathrm{MW} \\ 1, & 3.6\mathrm{MW} < P_{WT} \leq 10\mathrm{MW} \\ 1.38, & 10\mathrm{MW} < P_{WT} \end{cases} \tag{10}$$

Installation days of substructure and turbine are investigated from the database reported by Lacal-Arántegui et al [58]. Fig. 19 shows the variation of installation days with turbine rated power for turbine and

Table 9
Coefficient of variance (CoV) of each parameter in the cost models.

Model parameter	Nomenclature	Equation	CoV	Figure	N	p
Wind turbine cost	C_{WT}	Eq. (3–1)	0.11	Fig. 12	11	0.93
Diameter of monopile	d_{ss}	do.	0.12	Fig. 13 (a)	30	0.95
Length of monopile	l_{ss}	do.	0.18	Fig. 13 (b)	30	1.00
Thickness of monopile	t_{ss}	do.	0.27	Fig. 13 (c)	30	0.85
Cost of steel	$c_{ss,steel}$	do.	0.14	–	17	0.85
Cost of copper	c_{AC}, c_{EC}	Eqs. (3-3-1), (3-3-3)	0.18		17	0.48
Export cable length for nearby landfall point	$l_{EC,near}$	Eq. (3-3-1)	0.12	Fig. 14 (a)	18	0.40
Export cable length for distant landfall point	$l_{EC,far}$	do.	0.23	Fig. 14 (b)	12	0.98
Array cable length	l_{AC}	Eq. (3-3-3)	0.33	Fig. 17 (b)	30	0.18
Vessel fuel cost	$C_{vessel,fuel,i}$	Eq. (4-1-2)	0.27	–	17	0.80
Vessel size factor of turbine less than 3.6 MW	$A_{vessel,WT}$	Eq. (4-1-3)	0.43	Fig. 18 (a)	8	0.63
Vessel size factor of turbine more than 3.6 MW	do.	do.	0.23	do.	11	0.05
Vessel size factor of substructure less than 3.6 MW	$A_{vessel,SS}$	do.	0.38	Fig. 18 (b)	12	0.13
Vessel size factor of substructure more than 3.6 MW	do.	do.	0.25	do.	10	0.57
Installation days of wind turbine	$T_{install,WT}$	do.	0.41	Fig. 19 (a)	56	0.10
Installation days of substructure	$T_{install,SS}$	do.	0.51	Fig. 19 (b)	56	0.27
Weather downtime	α	do.	0.03	Fig. 20 (b)	6	0.94

Table 10
Description of duration time and operational limits in each installation phase for UK wind farms [35].

	Installation phase	Installation duration time (hour)	Wind speed (m/s)	Significant wave height (m)
1	Dredging & survey	48	11	1.5
2	Foundation installation	48	12	2
3	Transition piece installation	24	12	2
4	Wind turbine installation	24.5	8	2
5	Scour protection	14.4	15	2.5
6	PLGR	14.4	20	2
7	Cable installation	31.7	15	1.5
8	Cable burial	36	12	3

substructure installations. Turbine and substructure installation days do not have a clear dependency on turbine rated powers, but the uncertainty is quite large since the installation methodology and weather condition may affect these installation data.

3.2.4. Evaluation of uncertainties in models

The uncertainties of parameters in the proposed model are evaluated using Equations (5)-(7) explained in Section 2.2.4. The predicted coefficient of variance is summarized in Table 9. The steel and copper material are evaluated based on the recorded time series data [59,60]. The number of samples and the p value of Kolmogorov-Smirnov test using significance level of 0.05 are also described. It is found that all parameters follow the normal distribution.

3.2.5. Workability assessment by discrete event simulation

The workability is assessed using time series data available at Borssele wind farm site [67] and is evaluated by the discrete event simulation for 20 years from 1992 to 2011. The installation phases and its required installation duration time, limited wind speed and significant wave height are summarized in Table 10 as surveyed by Paterson et al. [35]. Fig. 20 (a) shows the annual average of workability and. Fig. 20 (b) shows the relationship between the coefficient of variance of workability and number of installation year. The variation of workability significantly decreases when the construction period is longer than 3 years.

3.2.6. Validation of the proposed probabilistic engineering cost model

CAPEX is evaluated using the proposed probabilistic engineering cost model for each offshore wind farm in the UK. The predicted mean value of each wind farm by the proposed and conventional cost models are plotted in Fig. 21 (a). The predicted mean value for each offshore wind farm by the proposed model match well with the reported data and capture the increase and decrease of CAPEX in the UK due to the technology transition such as increases of vessel size and turbine rated power, while the parametric model cannot reproduce the increase and decrease of CAPEX. The predicted standard deviation of each wind farm is plotted in Fig. 21 (b). The standard deviation shows the same trend as the mean value.

Fig. 22 (a) shows the reported and predicted CAPEX by the proposed engineering cost model and parametric cost model for the UK offshore wind farm with monopile foundations to validate the proposed engineering cost model. The mean value of CAPEX for 30 offshore wind farms is evaluated using Equations (11) - (12).

$$\mu_{actual} = \frac{\sum x_{actual,i}}{N_{farm}} \tag{11}$$

$$\mu_{model} = \frac{\sum x_{model,i}}{N_{farm}} \tag{12}$$

where, $x_{actual,i}$ is the reported CAPEX and $x_{model,i}$ is the predicted CAPEX by the proposed engineering cost model and the parametric model for wind farm i. N_{farm} is the number of wind farms.

It is obvious that the parametric model underestimates the reported CAPEX, since it cannot capture the technological development such as increases of vessel size and turbine rated power. On the other hand, the predicted CAPEX by the proposed engineering cost model agrees well with the reported CAPEX. The prediction error in mean value is reduced from 27.7 % to 2.3 %.

The reported standard deviation of CAPEX for 30 offshore wind farms is evaluated using Equations (13), that is, the standard deviation is calculated from the predicted mean value of CAPEX $\bar{x}_{model,i}$ and the reported CAPEX $x_{actual,i}$ for i th wind farm. The uncertainty predicted by the proposed model is evaluated using Equation (14). The predicted CAPEX $x_{model,i}$ for i th wind farm is evaluated by the proposed model considering the uncertainty of i th wind farm.

$$\sigma_{actual} = \sqrt{\frac{\sum \left(x_{actual,i} - \bar{x}_{model,i}\right)^2}{N_{farm}}} \tag{13}$$

$$\sigma_{model} = \sqrt{\frac{\sum \left(x_{model,i} - \bar{x}_{model,i}\right)^2}{N_{farm}}} \tag{14}$$

Fig. 22 (b) shows the reported and predicted standard deviation of CAPEX. The bar in the proposed model shows the standard deviation obtained from 50 calculation trials. The conventional parametric model

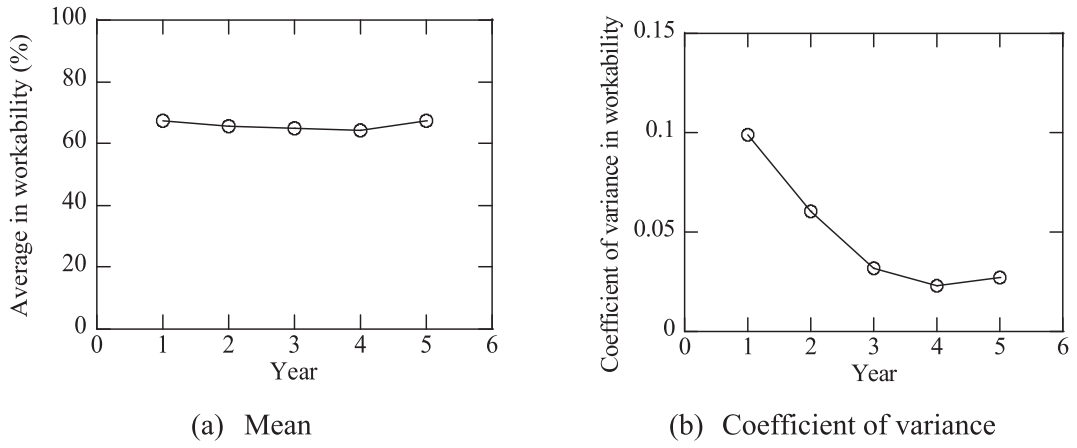

Fig. 20. Sensitivity of workability with installation years.

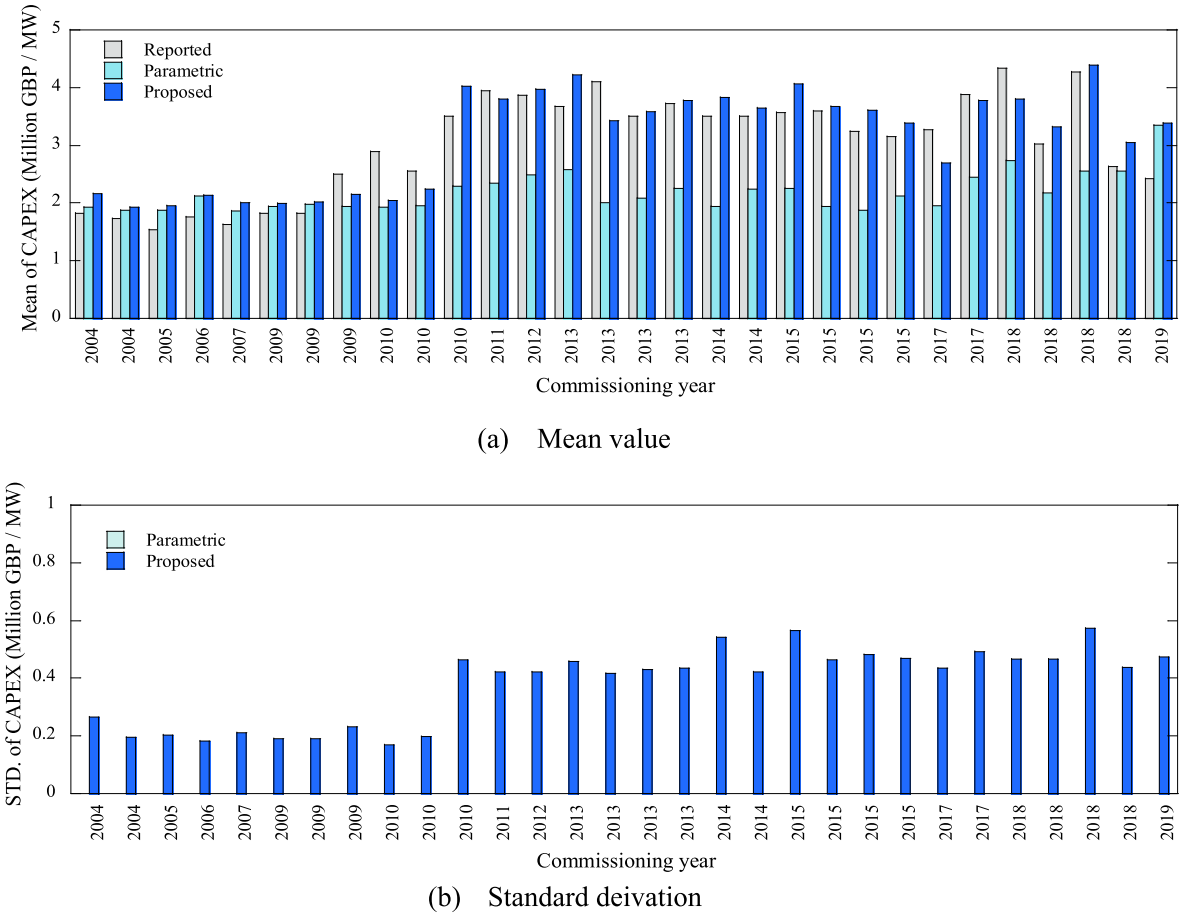

Fig. 21. Comparison of mean and standard deviation of CAPEX reported in the UK and predicted by the proposed probabilistic engineering cost model and the parametric cost model.

cannot predict the standard deviation of CAPEX, while the proposed probabilistic engineering cost model shows the reasonable standard deviation of CAPEX The prediction error in standard deviation is reduced from 100 % to 13 %.

3.3. Cost reduction scenarios of offshore wind in Japan

The cost reduction of offshore wind at different phases in Japan is analyzed using the proposed engineering cost model. Table 11 shows the comparison of LCOE between UK and Japan. The values in the UK is referred from the document by Catapult [68]. The capacity factor in the UK is 50 % and that in Japan is 33.2 %, which corresponds that the annual average of wind speed is 10 m/s in the UK and 7.5 m/s in Japan. CAPEX and OPEX in Japan are about 1.5 to 1.7 times larger than those in the UK. Referring the cost reduction mechanism in the UK as described in Section 3.1, the cost reduction scenarios in Japan are proposed to aim at the LCOE reduction from 20 JPY/kWh to 8–9 JPY/kWh. Three cost reduction phases are discussed and summarized in Table 12. Note that

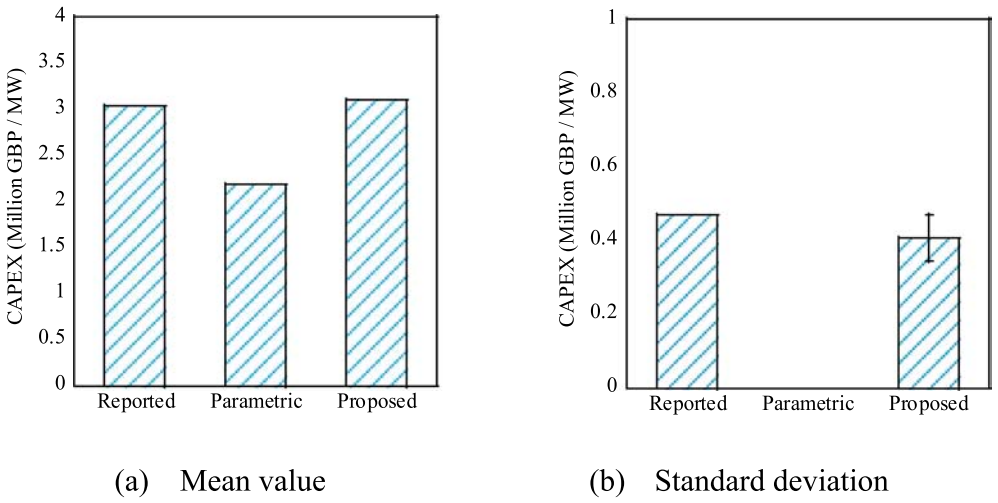

Fig. 22. Comparison of reported and predicted CAPEX by the parametric model [9] and the proposed engineering model.

Table 11
Comparison of LCOE in the UK and Japan in 2020.

Cost element	UK	Japan
CAPEX	32.6 M JPY/MW	51.2 M JPY/MW
OPEX	1.04 M JPY/MW/Year	1.84 M JPY/MW/Year
DECEX	4.2 M JPY/MW	10.7 M JPY/MW
FCR	4.67 %	3 %
Operational year	25 years	20 years
Availability	97 %	95 %
Capacity factor	50 %	33.2 %
LCOE	7 JPY/kWh	20 JPY/kWh

Table 12
Description of cost reduction phases in Japan.

Phase	Description	Evidence
Baseline	Cost assessment with the current technology 37 turbines of 10 MW	Government assessment in 2019 [3]
Phase 1	Prepare the specific offshore wind farm installation vessel and the installation time reduces to European level and use the turbine with a rated power ranged from 8 to 10 MW.	The industry announcements by Shimizu Ltd., Obayashi Ltd., and Kajima Ltd. [69–71]
Phase 2	Enlarge the turbine rated power from 12 MW to 15 MW	The range of 8 – 15 MW is considered and announced for offshore wind farm [72–74]
Phase 3	Operation and maintenance efficiency improvement	Japan onshore and offshore wind farm practice [75]

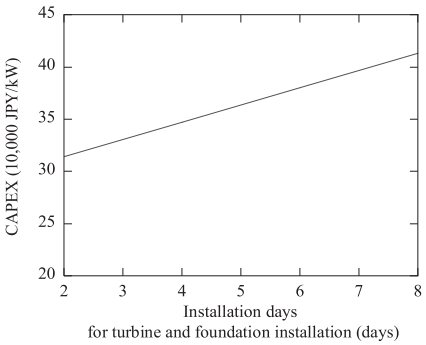

Fig. 23. Sensitivity of predicted CAPEX with installation days.

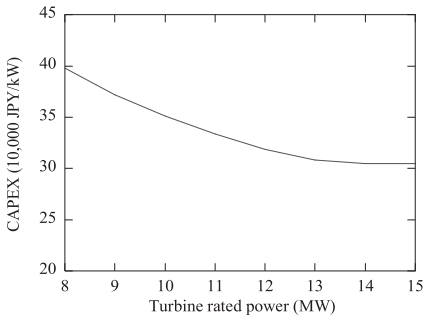

Fig. 24. Sensitivity of predicted CAPEX with turbine rated power.

the cost model is based on the engineering principles and the safety is secured in the cost reduction.

As to Phase 1, the construction efficiency is improved with advanced installation vessels. In Japan, some construction companies are building the specific self-elevated platform vessels for offshore wind farm installation [69–71] and the first one will start to operate in 2023, and work at a site with swells around 10 s. The 8 – 10 MW wind turbines are used in the offshore wind projects in the port area [76,77]. In order to clarify the effct of instolltion days on CAPEX, a sensitivity study of CAPEX is conducted using the proposed engineering cost model. A baseline wind farm is set as 10 MW of turbine rated power, 40 turbines, 10 km far from the coast and 20 m water depth. In this sensitivity study, no offshore substation is assumed. As expected, the installation days of one turbine and foundation has a very large impact, where the CAPEX increases 4 % for one more installation day as shown in Fig. 23.

In Phase 2, the turbine size is enlarged from 12 MW to 15 MW. 8 MW to 12.6 MW turbines were considered in the first auction according to the Environmental Impact Assessment documents [72,73] and 15 MW wind turbine was already announced to be released by a turbine manufacture [74]. The vessels with 2,500 ton crane capacity was planned to install 3 turbines of 12 MW in 5 days [69]. As expected, the impact of turbine rated power has a large impact. The CAPEX reduces 25 % from 8 MW turbine to 15 MW turbine as shown in Fig. 24.

Regarding to Phase 3, the OPEX is reduced. The study of OPEX reduction for onshore wind energy in Japan was conducted by Kikuchi and Ishihara [75] and the cost is reducedfrom 9,300 JPY/kW to 4,603 JPY/kW with spare part management, condition-based maintenance and operation and maintenance (O&M) efficiency improvement with matured experience. The availability is also improved from 87.4 % to 96.4 %. The same cost reduction ratio of onshore wind is adopted to

Table 13
Predicted LCOE for different phases at the representive site in Japan Sea side area.

Phase Description		Reference Current technology	Phase 1 Construction efficiency	Phase 2 Turbine enlargement	Phase 3 O&M efficiency
CAPEX	(JPY/kW)	51.2	38.0	33.2	26.7
OPEX	(JPY/kW/yr)	1.84	1.84	1.84	1.40
DECEX	(JPYY/kW)	20.2	11.0	8.0	3.5
WACC	(%)	6.12	6.12	6.12	6.12
Operation year	(Year)	20	20	20	20
Availability	(%)	95	95	95	97
Capacity factor	(%)	33.2	33.2	33.2	33.9
LCOE	(JPY/kWh)	20	17.0 ± 1.4	13.6 ± 1.1	10.1 ± 0.9
Reduction rate	(%)	–	15.0	32.2	49.4

Table 14
Predicted supply price for different phases at sites faced to Japan Sea.

		Reference	Phase 1	Phase 2	Phase 3
Commission year		2020	2024–2026	2026–2028	2028–2030
IRR	(%)	10 %	10 %	8 %	6 %
Expected Supply price	(JPY/kWh)	29.0	23.6 ± 2.2	17.4 ± 1.7	11.9 ± 1.1

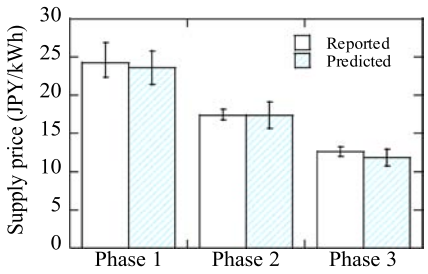

Fig. 25. Comparison of predicted and reported supply price at the first auction in Akita prefecture.

offshore wind farm in this study.

The calculated LCOE and its standard deviation using the proposed probabilistic engineering cost model for each phase are summarized in Table 13. The LCOE reduces from 20 Yen/kWh to 16 JPY/kWh, 13 JPY/kWh, 10 JPY/kWh in Phase 1, 2, 3, respectively. If the operation year extends from 20 years to 25 years by the law amendment in Japan, the predicted LCOE can be reduced to 9 JPY/kWh, which corresponds to the governement target for cost reduction of offshore wind.

The supply price and its standard deviation are calculated based on the predicted LCOE in Table 13 with the assumed Internal Rate of Return (IRR) described in Table 14. Reference model assumes IRR as 10 % acoording to the government announcement, which reflects the higher risk in the initial phase of the offshroe wind development. The IRR is assumed to decrease with later commissioning years because the risk will decreases.

The predicted supply prices for the three offshore wind farms are compared with the supply prices reported at the first auction on December 25, 2021 [78] to examine the proposed scenarios at various phases. Two wind farms are located in Akita prefecture and one in Chiba prefecture. 10 consortia participated in the Akita auction and two consortia participated in the Chiba auction. If the same consortium participates in auctions on two sites, it will be counted as two participants. Reported supply prices are grouped according to three phases based on the proposed supply price and the commissioning year.

Fig. 25 shows the comparison of predicted and reported supply price at the first auction in Akita prefecture. Bars indicate the standard deviation of the reported supply prices across different participants. It is found that the predicted supply prices in each phase correspond to the reported supply prices at the first auction. The highest supply price group corresponded to Phase 1, where 8–10 MW wind turbines and advanced installation vessels were proposed, with commissioning years from 2024 to 2026. The middle supply price group matched to Phase 2, which used 12–14 MW wind turbines and advanced installation vessels, with a commissioning year envisaged from 2026 to 2028. The lowest supply price group reached Phase 3, where an advanced OPEX strategy was added and the commissioning year was planned from 2028 to 2030.

The reported supply price through the first auction for the site in Chiba prefecture is about 1.3 time higher than that in Akita prefecture. Two consortia attended both auctions in Akita and Chiba prefectures. The ratios of the proposed supply prices in the two prefectures for each consortium are calculated. In order to clarify this price difference, the workability and geological condition at Akita and Chiba sites are investigated as shown in Fig. 26. Fig. 26 (a) shows the calculated workability at Akita and Chiba sites by the discrete event simulation.

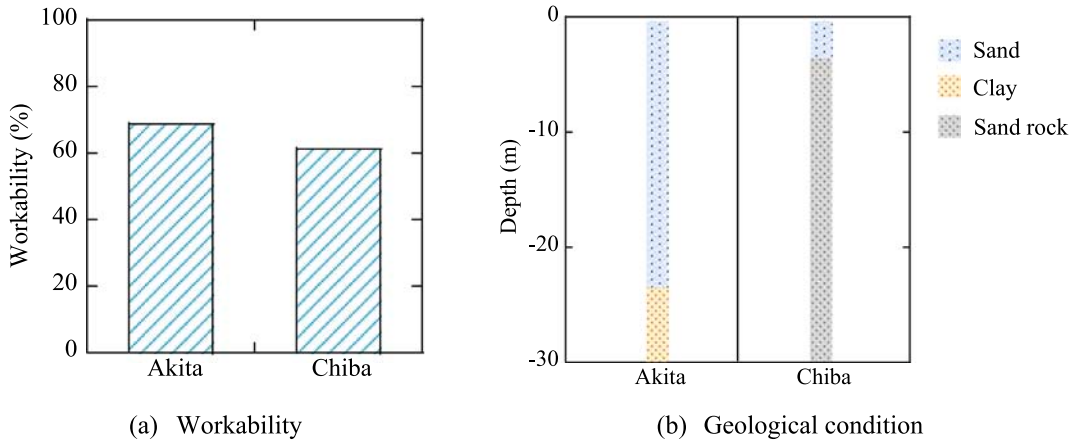

Fig. 26. Comparison of workability and geological condition at Akita and Chiba sites.

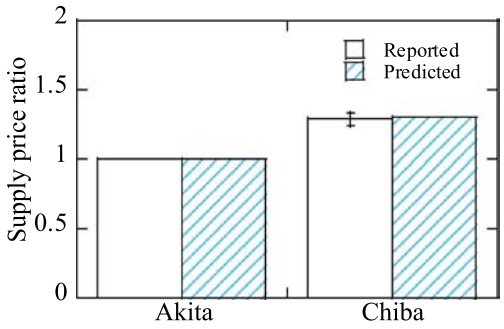

Fig. 27. Comparison of predicted and reported supply price ratios at Akita and Chiba sites.

The wind speeds and significant wave heights at two sites are calculated by WRF [38] and Wave Watch III for six years. The predicted workability of Akita site is 68 % and that of Chiba site is 61 %. Akita prefecture is located in the Japan Sea side and Chiba prefecture is faced to the Pacific Ocean, which means that the Chiba site has severer weather conditions. The geological conditions are also investigated based on the report of the boring test from the government at the Akita site [79] and the existing report of the boring test at the Chiba site [80]. The Akita site has thick sand and clay layers, while the Chiba site has more than 30 m sand rock layer, which takes more time to install a monopile as shown in Fig. 26 (b).

Fig. 27 shows the comparison of the predicted and reported supply price ratios at Akita and Chiba sites calculated using the proposed engineering cost model considering the differences of workability and installation days at two sites. The predicted supply price ratio is about 1.3 and agrees well with the reported one at the first auction. The difference of supply price between Akita and Chiba sites can be explained by the differences in workability and geological condition at two sites.

4. Conclusions

In this study, a probabilistic engineering cost model is proposed for fixed-bottom offshore wind farms. CAPEX of the UK offshore wind farms is assessed using the proposed model and validated by the collected database. The cost reduction scenario and its uncertainty of the offshore wind farms in Japan is analyzed and validated by the first auction. The following conclusions are obtained:

(1) The probabilistic engineering cost model is proposed to predict the mean value and standard deviation of CAPEX for offshore wind farms. A new export cable length model is proposed considering the landing point distance and the vessel size model is also proposed as the function of turbine rated power. The proposed engineering cost model succeeds in explaining the mechanism of CAPEX increase in the consolidation phase and CAPEX decrease in industrialization phase.
(2) The parameters and its uncertainty of the proposed probabilistic engineering cost model are identified from the reported data. The workability and its uncertainty are assessed by the discrete event simulation. The predicted mean value and standard deviation of CAPEX for the UK offshore wind farms with the monopile foundations show a good agreement with the reported those, while the conventional parametric model underestimates the mean value after the consolidation phase and cannot predict the uncertainty.
(3) The cost reduction scenarios and their uncertainties of offshore wind farms in Japan are analyzed using the proposed probabilistic engineering cost model. The levelized cost of wind energy can be reduced from 20 JPY/kWh to 17 JPY/kWh, 13.6 JPY/kWh and 10.1 JPY/kWh by the reduction of installation days, the turbine enlargement, the improvement of operation and maintenance efficiency. The predicted supply prices for each cost reduction scenario agree well with those reported at the first auction in Japan. The difference of supply price between Akita and Chiba sites is explained by the proposed cost model.

In this study, data used to determine the probability distribution of model parameter are limited, validation and improvement need to be further investigated.

Funding

This research received no external funding.

Data Availability Statement

The data in this research is not available.

CRediT authorship contribution statement

Yuka Kikuchi: Conceptualization, Methodology, Validation, Formal analysis, Investigation, Data curation, Writing – original draft, Writing – review & editing. **Takeshi Ishihara:** Conceptualization, Methodology, Visualization, Supervision, Project administration, Funding acquisition.

Declaration of Competing Interest

The authors declare that they have no known competing financial interests or personal relationships that could have appeared to influence the work reported in this paper.

Data availability

The authors do not have permission to share data.

Acknowledgments

This research is carried out as part of a joint program for next generation energy infrastructure with MHI Vestas Japan, J-POWER, Shimizu Corporation, Toshiba Energy Systems & Solutions Corporation, Class NK. The authors express their deepest gratitude to the concerned parties for their assistance during this study.

References

[1] Ministry of Environment, Study of potential for the introduction of renewable energy (FY2010) Summary, 2011. https://www.env.go.jp/earth/report/h23-03/summary_en.pdf (accessed on 15 January 2023).
[2] Public-private council on enhancement of industrial competitiveness for offshore wind power generation, overview of the vision for offshore wind power industry (1th), 2020. https://www.enecho.meti.go.jp/category/saving_and_new/saiene/yojo_furyoku/dl/vision/vision_first_overview_en.pdf (accessed on 15 January 2023).
[3] Procurement price calculation committee, Maximum amount of supply price in guidelines for public tender of exclusive occpancy and use of marine renewable energy power generation facilities (in Japanese), 2020, https://www.meti.go.jp/shingikai/santeii/pdf/059_b01_00.pdf (accessed on 15 January 2023).
[4] Smart G, Smith A, Warner E, Sperstad I, Prinsen B, Lacal-Arántegui R. Offshore wind farm baseline documentation. Technical report, IEA Wind Task 26; 2016, NREL/TP-6A20-66262. https://www.nrel.gov/docs/fy16osti/66262.pdf (accessed on 15 January 2023).
[5] The Crown Estate, A guide to an offshore wind farm. London, 2010. https://bvgassociates.com/cases/guide-offshore-wind-farm/ (Accessed on 15 January 2023).
[6] The Crown Estate and the Offshore Renewable Energy Catapult, A guide to an offshore wind farm: Updated and extended, 2019. https://www.thecrownestate.co.uk/media/2861/guide-to-offshore-wind-farm-2019.pdf (accessed on 15 January 2023).
[7] Ministry of Economy Trade and Industry, Basic research project on accelerating deplogyment of new energy: Study of wind energy potentail, 2011. (In Japanese).
[8] Fingersh L, Hand M, Laxson A. Wind Turbine Design Cost and Scaling Model. Technical report, National Renewable Energy Laboratory, 2006;29:1–43. https://www.nrel.gov/docs/fy07osti/40566.pdf (accessed on 15 January 2023).
[9] European Environment Agency, 2009, Europe's onshore and offshore wind energy potential: An assessment of environmental and economic constraints. European

Union, European Environment Agency Copenhagen, Denmark: European Environment Agency. https://doi.org/10.2800/11373 (accessed on 15 January 2023).
[10] Gonzalez-Rodriguez AG. Review of offshore wind farm cost components. Energy Sustain Dev 2017;37:10–9. https://doi.org/10.1016/j.esd.2016.12.001.
[11] Shafiee M, Brennan F, Espinosa IA. A parametric whole life cost model for offshore wind farms. Int J Life Cycle Assess 2016:961–75. https://doi.org/10.1007/s11367-016-1075-z.
[12] Alsubal S, Alaloul WS, Musarat MA, Shawn EL, Liew MS, Palaniappan P. Life cycle cost assessment of offshore wind farm: Kudat malaysia case. Sustain 2021;13. https://doi.org/10.3390/su13147943.
[13] Bayram S, Ocal ME, Laptali Oral E, Atis CD. Comparison of multi layer perceptron (MLP) and radial basis function (RBF) for construction cost estimation: the case of Turkey. J Civ Eng Manag 2016;22:480–90. https://doi.org/10.3846/13923730.2014.897988.
[14] Uncuoglu E, Citakoglu H, Latifoglu L, Bayram S, Laman M, Ilkentapar M, et al. Comparison of neural network, Gaussian regression, support vector machine, long short-term memory, multi-gene genetic programming, and M5 Trees methods for solving civil engineering problems. Appl Soft Comput 2022;129:109623. https://doi.org/10.1016/j.asoc.2022.109623.
[15] New Energy and Industrial Technology Development Organization (NEDO), Guidebook for introducing fixed-bottom offshore wind farm, 2018. (In Japanese).
[16] Akita Offshore Wind Corporation, https://aow.co.jp/en/eventa/pro_list.html (accessed on 15 January 2023).
[17] Fingersh L, Hand M, Laxson A. Wind turbine design cost and scaling model. Technical report, National Renewable Energy Laboratory; 2006, NREL/TP-500-40566. https://www.nrel.gov/docs/fy07osti/40566.pdf. (accessed on 15 January 2023).
[18] Kühn M., Bierbooms W.A.A.M., van Bussel G.J.W., Cockerill T.T., Harrison R., Ferguson M.C., et al. Towards a mature offshore wind energy technology—guidelines from the opti-OWECS project. Wind Energy 1999;2:25–58. https://onlinelibrary.wiley.com/doi/10.1002/(SICI)1099-1824(199901/03)2:1<3C25::AID-WE17>3E3.0.CO;2-8.
[19] Offshore Design Engineering Limited, Study of the costs of offshore wind generation: A report to the renewables advisory board (RAB) & DTI, Technical Report URN number 07/779, United Kingdom, Renewables Advisory Board (RAB) & DTI, 2007. https://www.osti.gov/etdeweb/biblio/21008017 (accessed on 15 January 2023).
[20] Department of trade and industry, The world offshore renewable energy report 2004-2008. 2004 Department of trade and industry, London. https://vbn.aau.dk/ws/files/50839429/The_World_Offshore_Renewable_Energy_Report_2004_2008_WD_part.pdf (accessed on 15 January 2023).
[21] Morgan C.A., Snodin H.M., Scott N.C. Offshore wind: economics of scale, engineering resource and load factors. 2003. Department of trade and industry, Bristol London. https://citeseerx.ist.psu.edu/viewdoc/download?doi=10.1.1.203.125&rep=rep1&type=pdf (accessed on 15 January 2023).
[22] Smart G, Offshore wind cost reduction: recent and future trends in the UK and Europe, Offshore Renewable Energy Catapult Report, TLI-SP-00007, 2016. https://ore.catapult.org.uk/analysisinsight/offshore-wind-cost-reduction/ (Accessed on 15 January 2023).
[23] Santhakumar S, Smart G, Noonan M, Meerman H. Technological Forecasting & Social Change Technological progress observed for fixed-bottom offshore wind in the EU and. UK 2022;182:121856. https://doi.org/10.1016/j.techfore.2022.121856.
[24] Jacquemin J, Butterworth D, Garret C, Baldock N, Henderson. A inventory of location specific wind energy cost, Spatial deployment of offshore wind energy in Europe (Wind-Speed). WP2 Report D2.2; 2011.
[25] Nielsen P Offshore wind energy projects feasibility study guidelines. SEAWIND-Altener project 4.1030/Z/01-103/2001, Ver. 3.0. Aalborg, Denmark; 2001.
[26] Dicorato M, Forte G, Pisani M, Trovato M. Guidelines for assessment of investment cost for offshore wind generation. Renew Energy 2011;36:2043–51. https://doi.org/10.1016/j.renene.2011.01.003.
[27] Ioannou A, Angus A, Brennan F. A lifecycle techno-economic model of offshore wind energy for different entry and exit instances. Appl Energy 2018;221:406–24. https://doi.org/10.1016/j.apenergy.2018.03.143.
[28] Nunemaker J., Shields M., Hammond R., Duffy P. ORBIT: Offshore Renewables Balance-of-system and Installation Tool, National Renewable Energy Laboratory, NREL/TP-5000-77081,2020. https://www.nrel.gov/docs/fy16osti/66579.pdf (accessed on 15 January 2023).
[29] Beiter P, Musial W, Smith A, Kilcher L, Damiani R, Maness M, et al. A spatial-economic cost-reduction pathway analysis for U.S. offshore wind energy development from 2015–2030. National Renewable Energy Laboratory, 2016. https://www.nrel.gov/docs/fy16osti/66579.pdf (accessed on 15 January 2023).
[30] Shields M, Beiter P, Nunemaker J, Cooperman A, Duffy P. Impacts of turbine and plant upsizing on the levelized cost of energy for offshore wind. Appl Energy 2021;298:117189. https://doi.org/10.1016/j.apenergy.2021.117189.
[31] Shields M, Beiter P, Kleiber W. Spatial impacts of technological innovations on the levelized cost of energy for offshore wind power plants in the United States. Sustain Energy Technol Assess 2021;45. https://doi.org/10.1016/j.seta.2021.101059.
[32] Gaglayan DG, Severin D, Heinrichs H, Linßen J, Stolten D, Robinius M. The techno-economic potential of offshore wind energy with optimized future turbine designs in Europe. Appl Energy 2019;255:113794. https://doi.org/10.1016/j.apenergy.2019.113794.
[33] Kaiser M J, Synder B F. Offshore wind energy cost modeling installation and decommissioning cost estimation in the U.S. outer continental shelf, U.S. Dept. of the Interior, Bureau of Ocean Energy Management, Regulation and Enforcement, Herndon, VA. TA&R study 648. 2010;340 pp. https://www.bsee.gov/sites/bsee.gov/files/tap-technical-assessment-program/648aa.pdf (accessed on 15 January 2023).
[34] Muhabie YT, Caprace J-D, Petcu C, Rigo P. Improving the installation of offshore wind farms by the use of discrete event simulation. World Marit Technol Conf. Providence, RI, USA. 2015:1–10. http://labsen.oceanica.ufrj.br/arq_publicacoes/improving-the-installation-of-offshore-wind-farms-by-the-use-of-discrete-event-simulation.pdf (accessed on 15 January 2023).
[35] Paterson J, D'Amico F, Thiles P, Kurt R, Harrison G. Offshore wind installation vessels – A comparative assessment for UK offshore rounds 1 and 2. Ocean Eng 2018;148:637–49. https://doi.org/10.1016/j.oceaneng.2017.08.008.
[36] Dewan A, Asgarpur M, Savenije R, Commercial proof of innovative offshore wind installation concepts using ECN Install Tool, 2015. http://resolver.tudelft.nl/uuid:91df978e-d3d3-4f14-810c-34eb4799aea1 (accessed on 15 January 2023).
[37] Shoreline, Shoreline Installation, 2020, https://docs.shoreline.io/installation (accessed on 2 September 2022).
[38] Kikuchi Y, Ishihara T. Assessment of weather window for the construction of offshore power plants using wind and wave simulations. J Phys Conf Ser 2016;753(9):1–11. https://doi.org/10.1088/1742-6596/753/9/092016.
[39] Kikuchi Y, Fukushima M, Ishihara T. Assessment of a coastal offshore wind climate by means of mesoscale model simulations considering high-resolution land use and sea surface temperature data sets. Atmosphere 2020;11(4):379. https://doi.org/10.3390/ATMOS11040379.
[40] Başakın EE, Ekmekcioğlu Ö, Çıtakoğlu H, Özger M. A new insight to the wind speed forecasting: robust multi-stage ensemble soft computing approach based on pre-processing uncertainty assessment. Neural Comput Appl 2022;34:783–812. https://doi.org/10.1007/s00521-021-06424-6.
[41] Muhabie YT, Rigo P, Cepeda M, de Almeida D'Agosto M, Caprace JD. A discrete-event simulation approach to evaluate the effect of stochastic parameters on offshore wind farms assembly strategies. Ocean Eng 2018;149:279–90. https://doi.org/10.1016/j.oceaneng.2017.12.018.
[42] Ozkan D, Financial analysis and cost optimization of offshore wind energy under uncertainty and in deregulated power markets, Doctoral thesis, The George Washington University, 2011. https://scholarspace.library.gwu.edu/etd/zw12z552r (accessed on 15 January 2023).
[43] Ioannou A, Angus A, Brennan F. Stochastic Prediction of Offshore Wind Farm LCOE through an Integrated Cost Model. Energy Procedia 2017;107:383–9. https://doi.org/10.1016/j.egypro.2016.12.180.
[44] The Crown Estate. Offshore wind cost reduction-Pathways study. 2012:1-88. https://www.thecrownestate.co.uk/media/1770/ei-offshore-wind-cost-reduction-pathways-study.pdf (Accessed on 15 January 2023).
[45] Catapult O.R.E. Floating Offshore Wind: Cost Reduction Pathways to Subsidy Free. Float Offshore Wind Cent Excell 2021;1–18. https://ore.catapult.org.uk/wp-content/uploads/2021/01/FOW-Cost-Reduction-Pathways-to-Subsidy-Free-report-.pdf (Accessed on 15 January 2023).
[46] Crown Estate Scotland ORE Catapult. Macroeconomic Benefits of Floating Offshore Wind in the UK. 2018:1-88. https://ore.catapult.org.uk/wp-content/uploads/2018/10/PN000244-FWMS-Report_FINAL.pdf (Accessed on 15 January 2023).
[47] 4C Offshore. Offshore wind farm online database. 2020, https://www.4coffshore.com/subscribers/dashboard/owf/onlinedb/windfarmodb.aspx. (Accessed on 15 January 2023).
[48] Sieros G, Chaviaropoulos P, Sorensen JD, Bulder BH, Jamieson P. Upscaling wind turbines: theoretical and practical aspects and their impact on the cost of energy. Wind Energy 2012;15:3–17. https://doi.org/10.1002/we.527.
[49] Smith A, Stehly T, Musial W. 2014-2015 Offshore Wind Technologies Market Report. National Renewable Energy Laboratory, 2015. https://www.nrel.gov/docs/fy15osti/64283.pdf (accessed on 15 January 2023).
[50] Moné C, Hand M, Bolinger M, Rand J, Heimiller D, Ho J. 2015 Cost of Wind Energy Review, NREL/TP-6A20-66861. National Renewable Energy Laboratory, 2017. https://www.nrel.gov/docs/fy17osti/66861.pdf (accessed on 15 January 2023).
[51] Stehly T, Heimiller D, and Scott G, 2016 Cost of Wind Energy Review, National Renewable Energy Laboratory, NREL/TP-6A20-70363, 2017. https://www.nrel.gov/docs/fy17osti/66861.pdf (accessed on 15 January 2023).
[52] Stehly T, Beiter P, Heimiller D, Scott G, 2017 Cost of Wind Energy Review, National Renewable Energy Laboratory, NREL/TP-6A20-72167, 2018. https://www.nrel.gov/docs/fy18osti/72167.pdf (accessed on 15 January 2023).
[53] Stehly T, Beiter P. 2018 Cost of Wind Energy Review, National Renewable Energy Laboratory, NREL/TP-5000-74598, 2019. https://www.nrel.gov/docs/fy20osti/74598.pdf (accessed on 15 January 2023).
[54] Stehly T, Beiter P, Duffy P, 2019 Cost of Wind Energy Review, National Renewable Energy Laboratory, NREL/TP-5000-78471, 2020. https://www.nrel.gov/docs/fy21osti/78471.pdf (accessed on 15 January 2023).
[55] Stehly T., Duffy P. Cost of Wind Energy Review, National Renewable Energy Laboratory, NREL/TP-5000-81209, 2021. https://www.nrel.gov/docs/fy22osti/81209.pdf (accessed on 15 January 2023).
[56] Negro V, López-Gutiérrez JS, Esteban MD, Alberdi P, Imaz M, Serraclara JM. Monopiles in offshore wind: Preliminary estimate of main dimensions. Ocean Eng 2017;133:253–61. https://doi.org/10.1016/j.oceaneng.2017.02.011.
[57] The Kingfisher Information Service – Offshore Renewable & Cable Awareness project, https://kis-orca.org/downloads/ (Accessed on 15 January 2023).
[58] Lacal-Arántegui R, Yusta JM, Domínguez-Navarro JA. Offshore wind installation: Analysing the evidence behind improvements in installation time. Renew Sustain Energy Rev 2018;92:133–45. https://doi.org/10.1016/j.rser.2018.04.044.
[59] U.S. Bureau of Labor Statics, Producer Price Index by Commodity: Metals and Metal Products: Hot Rolled Steel Sheet and Strip, Including Tin Mill Products,

https://fred.stlouisfed.org/series/WPU10170301#0 (Accessed on 15 January 2023).
[60] U.S. Bureau of Labor Statics, Producer Price Index by Commodity: Metals and Metal Products: Copper Wire and Cable, https://fred.stlouisfed.org/series/WPU10260314 (Accessed on 15 January 2023).
[61] U.S. Bureau of Labor Statics, Producer Price Index by Commodity: Fuels and Related Products and Power: Gasoline, https://fred.stlouisfed.org/series/WPU0571#0 (Accessed on 15 January 2023).
[62] The world bank, Databank, World development indicators, https://databank.worldbank.org/source/world-development-indicators (Accessed on 15 January 2023).
[63] Duffy A, Hand M, Wiser R, Lantz E, Dalla Riva A, Berkhout V, et al. Land-based wind energy cost trends in Germany, Denmark, Ireland, Norway, Sweden and the United States. Appl Energy 2020;277:114777. https://doi.org/10.1016/j.apenergy.2020.114777.
[64] van der Tempel J. Design of support structures for offshore wind turbines. Technical university of Delft; 2006. Doctoral thesis. http://resolver.tudelft.nl/uuid:ae69666e-3190-4b22-84ed-2ed44c23e670 (Accessed on 15 January 2023).
[65] Japan Wind Power Association, Installed capacity of wind power generation at the end of 2021, https://jwpa.jp/en/information/6227/ (Accessed on 15 January 2023).
[66] Ministry of Economy, Trade and Industry, "Offshore wind power generation" Progress since enforcement of the new law, https://www.enecho.meti.go.jp/en/category/special/article/detail_152.html (Accessed on 15 January 2023).
[67] Netherlands Enterprise Agency, Studies Borssele Wind Farm Sites IV, III & V: Metocean BWFZ – Time series Site IV – Deltares, https://offshorewind.rvo.nl/cms/view/4a3ea5ce-d027-4483-b471-00e5ed87a3bb/studies-borssele-iii-iv-v (Accessed on 15 January 2023).
[68] Catapult The benefits of hybrid bottom-fixed and floating wind sites; 2021. https://ore.catapult.org.uk/wp-content/uploads/2021/01/AI-paper-Floating-hybrid-sites-final-2021.01.11.pdf (Accessed on 15 January 2023).
[69] Shimizu corporation, "Shimizu begins construction of the world's largest self-propelled SEP (Self-elevating platform) vessel, https://www.shimz.co.jp/en/company/about/news-release/2019/2019007.html (Accessed on 15 January 2023).
[70] Obayashi corporation, "Obayashi begins construction of the SEP for offshore wind farm installation" (In Japanese), https://www.obayashi.co.jp/news/detail/news20180925_1.html (Accessed on 15 January 2023).
[71] Kajima corporation, KAJIMA integrated report, https://www.kajima.co.jp/english/sustainability/report/2020/pdf/ir_e_p20-51.pdf (Accessed on 15 January 2023).
[72] Tokyo Electric Power Company Holdings, Inc., Related to the offshore wind power generation business off the coast of Choshi: Planning stage environmental consideration book: Business explanation material (in Japanese), 2019. https://www.pref.chiba.lg.jp/kansei/eikyouhyouka/iinkai/documents/r010920_shiryo02_01.pdf (Accessed on 15 January 2023).
[73] Ministry of the Environment, Submission of the Minister of the Environment's Opinion on the Environmental Consideration Document at the Planning Stage for the Offshore Wind Power Generation Project off the Coast of Yurihonjo City, Akita Prefecture, 2020. https://www.env.go.jp/press/108281.html (Accessed on 15 January 2023).
[74] Vestas, V236-15MW. https://www.vestas.com/en/products/offshore/V236-15MW/V236-15MW (Accessed on 15 January 2023).
[75] Kikuchi Y, Ishihara T. Availability and LCOE analysis considering failure rate and downtime for onshore wind turbines in Japan. Energies 2021;14(12):3528. doi:10.3390/en14123528.
[76] Ministry of Land, Infrastructure, Transport and Tourism, Recent progress in promoting the introduction of offshore wind power (in Japanese), 2022, https://www.mlit.go.jp/policy/shingikai/content/001489039.pdf (Accessed on 15 January 2023).
[77] Hibiki Wind Energy Co. Hibiki Wind Energy Project Outline, http://hibikiwindenergy.co.jp/pdf/hwe_english.pdf (Accessed on 15 January 2023).
[78] Ministry of Economy, Trade and Industry, About the selection result of the offshore wind energy operator in 'Noshiro, Mitane-cho and Oga offshore site in Akita prefecture', 'Yurihojo in Akita prefecture', 'Choshi offshore in Chiba prefecture', https://www.meti.go.jp/press/2021/12/20211224006/20211224006.html (Accessed on 15 January 2023).
[79] Ministry of Economy, Trade and Industry, Ministry of Land, Infrastructure, Transport and Tourism and Akita prefecture, The 2nd council meeting about Akita Yurihonjo offshore site, (In Japanese), 2019, https://www.enecho.meti.go.jp/category/saving_and_new/saiene/yojo_furyoku/dl/kyougi/akita_yuri/02_docs04.pdf (Accessed on 15 January 2023).
[80] Chiba prefecture, geological database, https://www.pref.chiba.lg.jp/wit/chishitsu/chishitsudb.html (Accessed on 15 January 2023).